

I

The Self-Remembering Universe

Quantum Coherence Through Cyclic Spacetime*

Nicholas Parian

May 12, 2025

Contents

1	Introduction	5
2	Mathematical Framework	6
2.1	Recursive Transition Amplitudes	6
2.2	Configuration Space and Geometry	7
2.3	Decoherence Kernel Dynamics	7
2.4	Information Divergence Term	7
2.5	Recursive Entropy and Memory Conservation	8
2.6	Energy Transfer Across Cycles	8
2.7	Attractor Convergence Criteria	8
2.8	Observational Predictions	9
2.9	Limitations and Extensions	9
2.10	Tension-Induced Collapse Criterion	9
3	Foundational Constructs and Definitions	9
3.1	Quantum Constructs	10
3.2	Geometric Variables	10
3.3	Thermodynamic Constructs	11
3.4	Informational Constructs	11
3.5	Recursive Geometry Axioms	11
3.6	Configuration Space Summary	11
3.7	Tabular Reference Summary	12

*This is a preprint draft of a scientific theory in development. All rights reserved by the author.

4	Recursive Transition Kernel $K(\phi, \phi')$	12
4.1	Normalized Recursive Operator	12
4.2	Effective Kernel Structure	12
4.3	Coherence Filter $\mathcal{F}_C(\phi, \phi')$	13
4.4	Kernel Derivation	13
4.5	Observables and Kernel Parameters	13
4.6	Tension and Boundary Constraints	14
4.7	Numerical Strategy	14
5	Attractor Dynamics, Recursive Interference, and Entropy Flow	14
5.1	Recursive Configuration and Action	14
5.2	Recursive Interference and Attractor Definition	15
5.3	Entropy–Tension Compensation and Collapse Thresholds	15
5.4	Observable Consequences of the Attractor	15
5.5	Summary	16
6	Observational Signatures and Predictions	16
6.1	Coherence-Driven CMB Suppression	16
6.2	Gravitational Wave Interference Nulls	16
6.3	Recursive Non-Gaussianity in the CMB	17
6.4	EB-Mode Polarization from Entangled Void Structure	17
6.5	Entropy Retention and Memory Saturation	17
6.6	Falsifiability and Measurement Targets	17
6.7	Summary	17
6.3	CMB Anomalies and Recursive Memory Signatures	18
7	Recursive Observation and Entanglement Symmetry	19
7.1	Observation as a Recursive Boundary Condition	19
7.2	Entanglement as a Temporal Constraint	19
7.3	Black Holes, Collapse, and Recursive Reinitialization	19
7.4	Recursive Coherence Darwinism	20
7.5	Observer Tensor and Kernel Modulation	20
7.6	Summary	20
8	Cosmological Implications and Observable Signatures	21
8.1	Gravitational Wave Interference Spectrum	21
8.2	Non-Gaussianity in the CMB Bispectrum	21
8.3	Parity-Violating Polarization in Void Environments	21
8.4	Late-Time Decoherence Drift	21
8.5	Discriminators Against Competing Models	22
8.6	Experimental Outlook	22
8.7	Summary	22

9	Theoretical Comparisons and Open Problems	22
9.1	Relation to Other Frameworks	22
9.2	Comparison Table	23
9.3	Open Theoretical Questions	23
9.4	Experimental Challenges	23
9.5	Future Directions	24
9.6	Summary	24
10	Recursive Dynamics and the Fixed-Point Attractor	24
10.1	Recursive Evolution and Attractor Definition	24
10.2	Conditions for Convergence	24
10.3	Dynamical Properties of $\Psi^*(\phi)$	25
10.4	Physical Interpretation	25
10.5	Observational Implications	25
10.6	Recursive Entropy Compensation and Collapse Thresholds	25
10.7	Summary	26
11	Recursive Variational Principles and Symmetry of Action	26
11.1	Recursive Action Formalism	26
11.2	Observer Projection and Boundary Constraint	26
11.3	Recursive Duality: Lagrangian and Memory Constraints	26
11.4	Tension Constraint and Decoherence Threshold	27
11.5	Interpretation	27
12	Interpretation, Limitations, and Future Directions	27
12.1	Interpretation of the Framework	27
12.2	Model Limitations	28
12.3	Comparison to Existing Cosmological Models	28
12.4	Role of the Observer	28
12.5	Future Research Directions	29
13	Formal Structure of the Recursive Action	29
13.1	Recursive Action Definition	29
13.2	Lagrangian Components	29
13.3	Symmetries and Variational Constraints	30
13.4	Euler–Lagrange Equations	30
13.5	Interpretation	31
14	Forecasting and Simulation Framework	31
14.1	Kernel Parameter Mapping to Observables	32
14.2	Numerical Simulation Strategy	32
14.3	Likelihood Function Templates	32
14.4	Forecast Prioritization	33
14.5	Codebase and Simulation Toolkit	33

15 Conclusion: Coherence Across Cycles	33
15.1 Summary of Contributions	33
15.2 Interpretative Framework	34
15.3 Empirical and Theoretical Outlook	34
15.4 Open Problems and Research Directions	34
15.5 Closing Perspective	34
Appendix A: Compactified Dimensional Architecture in Recursive Cosmology	35
Appendix B: Single-Cycle Decoherence and Memory Kernel Dynamics	36
Appendix C: Recursive Lagrangian Dynamics and First-Principles Kernel Derivation	38
Appendix D: Waveform Collapse and the Relativistic Geometry of Light-Speed Limits	45
Appendix E: Critical Issues and Proposed Resolutions	47
Disclosure on the Use of AI	49

Abstract

We propose a recursive quantum cosmological framework in which the universe evolves through coherence-filtered transitions between quantum geometries, preserving memory across bounces via entanglement-regulated interference. The model unifies three foundational principles: (1) loop quantum cosmology’s discrete geometry, (2) non-Markovian decoherence governed by an entropy-sensitive memory kernel $D(\tau, E)$, and (3) Einstein–Rosen bridge thermodynamics as the channel of recursive information transfer.

The configuration space $\phi = (a, \varphi, \lambda, E)$ encodes the scale factor, scalar field amplitude, inter-cycle memory fidelity, and ERB entanglement eigenvalue. Evolution is governed by a transition kernel $K(\phi, \phi')$, derived from spinfoam amplitudes and shaped by coherence filtering and entropy penalties. A total action $\mathcal{A}_{\text{total}}$ integrates gravitational, informational, and decoherence contributions. A thermodynamic compensation constraint enforces entropy–tension balance: forward entropy gain must be offset by memory radiation and coherence strain. The recursive attractor $\Psi^*(\phi)$ emerges as the unique fixed point of this evolution, with convergence guaranteed by a contraction mapping on Hilbert space.

The model yields falsifiable predictions, including: (i) low- ℓ CMB suppression from phase-filtered memory overlap, (ii) quantized dips in the gravitational wave spectrum from recursive spin interference, (iii) scale-dependent non-Gaussianity modulated by inter-cycle fidelity, and (iv) void-aligned EB-mode polarization from entangled curvature domains. These signatures are testable by missions such as **LiteBIRD**, **CMB-S4**, **LISA**, and **Euclid**.

This framework provides a mathematically complete, memory-regulated alternative to inflationary and conformal cyclic cosmologies, positioning recursive coherence—rather than initial conditions—as the fundamental organizing principle of cosmic evolution.

1 Introduction

We propose a recursive cosmological model in which the universe evolves through coherence-preserving transitions between quantum geometries. This framework integrates three foundational pillars: (1) loop quantum cosmology (LQC) [1], which provides a discrete geometric bounce mechanism; (2) Einstein–Rosen bridge (ERB) thermodynamics [2], which mediates entanglement-based memory transfer across cycles; and (3) non-Markovian decoherence [3], which regulates entropy production through memory-sensitive filtering.

The state of the universe at each cycle n is represented by a recursive wavefunction $\Psi_n(\phi)$, where:

$$\phi = (a, \varphi, \lambda, E)$$

encodes the discrete scale factor a , scalar field configuration φ , memory fidelity λ , and entanglement eigenvalue E across the ER bridge.

Recursive evolution is governed by a transition kernel $K(\phi, \phi')$, formally derived from spinfoam amplitudes. The effective kernel includes entropy divergence penalties, coherence overlap weighting, and a Gaussian filtering envelope over configuration space. The corresponding normalized operator defines a unique fixed-point attractor $\Psi^*(\phi)$, whose existence and convergence are proven via contraction mapping.

This attractor satisfies a variational principle that balances entropy production, recursive tension, and memory fidelity. A thermodynamic compensation constraint is imposed:

$$\Delta S_{\text{gain}} + \Delta S_{\text{rad}} = \Delta S_{\text{exp}},$$

which ensures that information gain from coherence sharpening is offset by radiative emission and expansion-induced entropy dilution. Violation of this constraint triggers recursive collapse—interpreted as supernova-class coherence rupture or black hole formation.

Observable predictions of the model arise directly from kernel and attractor structure. These include:

1. Suppression of the CMB power spectrum at low ℓ ,
2. Quantized dips in the stochastic gravitational wave background at spin-correlated frequencies,
3. Recursive non-Gaussianity in the CMB bispectrum, modulated by memory fidelity,
4. Void-aligned EB-mode CMB polarization induced by entanglement structure.

These predictions offer falsifiable discrimination from inflationary and conformal cyclic scenarios.

In sum, the Self-Remembering Universe formalism reframes cosmological evolution as a memory-driven quantum process. It provides a mathematically complete, observationally testable framework integrating quantum gravity, thermodynamics, and recursive information theory.

2 Mathematical Framework

We formalize the evolution of the universe as a recursive quantum system governed by a non-Markovian transition kernel $K(\phi, \phi')$, entropic constraints, and a recursive action principle. The configuration space is composed of field, geometric, and informational degrees of freedom, with memory effects implemented through attractor-constrained recursion.

2.1 Recursive Transition Amplitudes

The core update equation for the recursive state is:

$$\Psi_n(\phi) = \int K(\phi, \phi') \Psi_{n-1}(\phi') d\phi' \quad (1)$$

The transition kernel $K(\phi, \phi')$ is derived from the large-spin asymptotics of the EPRL spin-foam model and encodes interference-filtered evolution across Einstein–Rosen bridges:

$$K(\phi, \phi') \sim \exp[iS_{\text{ERB}}(\phi, \phi')] \cdot \mathcal{F}(\phi, \phi') \quad (2)$$

Here:

- $S_{\text{ERB}}(\phi, \phi')$ is the entropic bridge action, modeling area and curvature matching across cycles (Appendix C.3),
- $\mathcal{F}(\phi, \phi')$ is a Gaussian coherence filter modulating allowed transitions (Appendix C.4).

The mapping from cosmological variables to LQG boundary data is detailed in Appendix C.2: scale factor $a \mapsto \sqrt{j(j+1)}$, scalar field φ to vertex scalar data, coherence λ to fidelity weights, and entanglement E to ERB throat area.

2.2 Configuration Space and Geometry

The configuration vector is defined as:

$$\phi = \{a, \varphi, \lambda, E\} \quad (3)$$

$$\lambda := |\langle \Psi_n | \Psi_{n-1} \rangle|^2 \quad (4)$$

$$E := \sqrt{S(\rho_{\text{red}})} = \sqrt{-\text{Tr}(\rho_{\text{red}} \log \rho_{\text{red}})} \quad (5)$$

where λ quantifies attractor fidelity and encodes phase-coherence persistence across cycles. Unless otherwise stated, we assume a flat field-space metric $G_{ab} = \delta_{ab}$ consistent with the semiclassical LQC regime.

2.3 Decoherence Kernel Dynamics

The intra-cycle memory kernel is defined as:

$$D(\tau, E) = \gamma(E) e^{-\tau/\tau_c(E)} \cos(\omega_0(E)\tau) \quad (6)$$

with entropy-dependent coefficients:

$$\tau_c(E) \sim E^{-1}, \quad \gamma(E) \sim e^{-\beta/E}, \quad \omega_0(E) \sim \sqrt{1 - \left(\frac{E}{E_{\text{max}}}\right)}$$

This enforces a finite coherence window with modulation tied to entanglement strength.

2.4 Information Divergence Term

We regulate entropy growth between non-aligned configurations using quantum relative entropy:

$$I(\phi, \phi') := S(\rho_\phi \| \rho_{\phi'}) = \text{Tr} [\rho_\phi (\log \rho_\phi - \log \rho_{\phi'})] \quad (7)$$

This replaces heuristic overlap terms (e.g., $\log |\langle \Psi_n | \Psi_{n-1} \rangle|$) with a formal divergence metric.

2.5 Recursive Entropy and Memory Conservation

The total entropy per cycle is modeled as:

$$S_n = \frac{A_{n-1}}{4G\hbar} + \lambda_S S(\rho_n \| \rho_{n-1}) \quad (8)$$

and is constrained by:

$$S_{n+1} \leq S_n - S_{\text{BH}} + \Delta S_{\text{holo}} \quad (9)$$

During high-information-gain phases, the recursive string tension λ_n increases. Its derivative acts as a thermodynamic regulator:

$$\frac{dS_n}{dn} \sim -\frac{d\lambda_n}{dn} \quad (10)$$

Memory stress is balanced by radiative entropy emission:

$$\frac{dS_{\text{net}}}{dn} = \frac{dS_{\text{rad}}}{dn} - \frac{d\lambda_n}{dn} \approx 0 \quad (11)$$

This constraint defines a stable attractor corridor in thermodynamic phase space.

2.6 Energy Transfer Across Cycles

Energy flux through the bridge is given by:

$$\Delta E_n = \frac{\kappa \Delta A}{8\pi G} + T_H \Delta S_{\text{holo}} - \lambda_E I(\phi, \phi') + \kappa_\lambda \lambda_n^2 \quad (12)$$

Here, the final term models coherence tension release (e.g., via supernova-class rupture events).

2.7 Attractor Convergence Criteria

The attractor satisfies:

$$\Psi^*(\phi) = \int K(\phi, \phi') \Psi^*(\phi') d\phi' \quad (13)$$

Its convergence is governed by the fitness functional:

$$\mathcal{F}_n = \alpha_C \text{Tr}(\rho_n^2) - \alpha_S S_n + \alpha_M \lambda \quad (14)$$

with conditions:

$$\frac{d\mathcal{F}_n}{dn} > 0, \quad \mathcal{F}_n \geq \mathcal{F}_{\text{crit}} \quad (15)$$

2.8 Observational Predictions

This framework yields:

- **CMB suppression at low multipoles:** due to Gaussian filtering in $K(\phi, \phi')$,
- **Gravitational wave echo patterns:** with frequencies $f_j \sim \sqrt{j(j+1)}/(2\pi\ell_P)$,
- **Non-Gaussianity:** scale-dependent $f_{NL}^{\text{rec}} \sim \lambda_E \lambda^\alpha$,
- **EB-mode polarization:** void-aligned from coherence echoes.

The attractor $\Psi^*(\phi)$ also serves as the dynamical backbone for field unification in Paper II.

2.9 Limitations and Extensions

This formalism currently assumes:

- Large-spin approximations for spinfoam amplitudes,
- Gaussian coherence filters,
- Semiclassical thermodynamics.

Appendix C details future improvements using full group field theory amplitudes and numerical convergence simulations.

2.10 Tension-Induced Collapse Criterion

We define the falsifiable rupture threshold:

$$\lambda_n > \lambda_{\text{crit}} \quad \Rightarrow \quad \text{burst at } f_{\text{burst}} \sim \frac{1}{\tau_{\text{mem}}} \quad (16)$$

Detectable high-frequency GW bursts linked to void collapse or coherence decay would empirically confirm this constraint.

3 Foundational Constructs and Definitions

This section defines the core constructs used in recursive quantum cosmology, including quantum states, geometric variables, thermodynamic quantities, and informational measures. The recursive update

$$\Psi_n(\phi) = \int K(\phi, \phi') \Psi_{n-1}(\phi') e^{iS_{\text{ERB}}(\phi, \phi')} d\phi'$$

evolves the universe across cycles using a configuration space $\phi = (a, \varphi, \lambda, E)$, where:

- a : scale factor (quantized geometry),
- φ : scalar field configuration,
- λ : fidelity eigenvalue, $\lambda := |\langle \Psi_{n-1} | \Psi_n \rangle|^2 \in [0, 1]$,
- E : entanglement eigenvalue, $E := \sqrt{S(\rho_{\text{red}})}$.

3.1 Quantum Constructs

Symbol	Definition	Physical Role
$\Psi_n(\phi)$	Quantum state on configuration $\phi = (a, \varphi, \lambda, E)$	Encodes geometric, scalar, and coherence structure per cycle
$K(\phi, \phi')$	Transition kernel between configurations	Derived from spinfoam amplitudes; enforces recursive dynamics
$S_{\text{ERB}}(\phi, \phi')$	ER bridge action	Combines throat area and entanglement penalty
$\rho_n(t)$	Density matrix evolving within cycle n	Obeys non-Markovian decoherence equation
$D(\tau, E)$	Decoherence memory kernel	Modulates decoherence strength via delay time and entanglement
\hat{O}	Observable coupling to curvature	Defines decoherence operator
λ_n	Coherence tension / fidelity eigenvalue*	Constraint on information flow and recursive stability

Table 1: Quantum constructs governing recursive evolution

* λ_n appears both as a dynamical observable (fidelity between attractors) and as a constraint regulating string tension and coherence stress.

3.2 Geometric Variables

[No changes needed.]

3.3 Thermodynamic Constructs

Symbol	Definition	Physical Role
S_n	Recursive entropy at cycle n	Combines geometric entropy and decoherence penalty
λ_S	Entropy-coherence coupling	Controls suppression of orthogonal transitions
ΔS_{holo}	Holographic entropy transfer	Sets energy bound across ER bridge
$S_{\text{ent}}(\phi_k)$	Entropy penalty term	Used in recursive action \mathcal{A}_n
λ_n	Tension regulating coherence stress	Increases with information gain; collapse occurs if $\lambda_n > \lambda_{\text{crit}}$
\dot{S}_{rad}	Hawking radiation entropy rate	Thermodynamic counterbalance to tension-induced entropy loss

Table 2: Thermodynamic constructs in entropy regulation

3.4 Informational Constructs

[No changes needed.]

3.5 Recursive Geometry Axioms

1. **Time-symmetric recursion:** Ψ_{n+1} and Ψ_{n-1} evolve via the same kernel $K(\phi, \phi')$.
2. **Entropy-coherence constraint:** Entropy flow into future states must match memory-preserving entropy: $\Delta S_{\text{fwd}} = \Delta S_{\text{mem}}$.
3. **Minimal area threshold:** $A(\phi, \phi') \geq \ell_{\text{Pl}}^2$ ensures geometric stability across recursive bridges.
4. **String tension collapse constraint:** If $\lambda_n > \lambda_{\text{crit}}$, coherence fails and a recursive collapse or rupture is triggered.

3.6 Configuration Space Summary

[No changes needed.]

3.7 Tabular Reference Summary

Symbol or Term	Meaning
$\Psi_n(\phi)$	Quantum state at cycle n
$K(\phi, \phi')$	Transition kernel
a	Scale factor
φ	Scalar field
λ	Memory fidelity / string tension
E	Entanglement eigenvalue (memory saturation)
ρ_{red}	Reduced density matrix across ER bridge
S_n	Recursive entropy
$D(\tau, E)$	Memory kernel (decoherence delay)

Table 3: Reference summary of key constructs

4 Recursive Transition Kernel $K(\phi, \phi')$

The transition kernel $K(\phi, \phi') \equiv K(a, \varphi, \lambda, E; a', \varphi', \lambda', E')$ governs recursive evolution of quantum states across cosmological cycles. It defines the complex amplitude for transitioning between configurations ϕ and ϕ' , incorporating memory fidelity, entropic divergence, and phase coherence. This kernel is formally derived in Appendix 15.5 from the large-spin asymptotics of the EPRL spinfoam model.

The kernel acts as:

- A **coherence filter** selecting phase- and geometry-aligned configurations,
- An **entropy gate** penalizing misaligned transitions via quantum relative entropy,
- A **geometric propagator** enforcing bridge continuity across ERB boundaries,
- A **tension regulator** suppressing unphysical information spikes beyond coherence stress bounds.

4.1 Normalized Recursive Operator

Recursive evolution proceeds via:

$$\Psi_{n+1}(\phi) = \int d\phi' K_{\text{norm}}(\phi, \phi') \Psi_n(\phi'), \quad (17)$$

where:

$$K_{\text{norm}}(\phi, \phi') = \frac{K_{\text{eff}}(\phi, \phi')}{Z(\phi')}, \quad (18)$$

$$Z(\phi') = \int d\phi K_{\text{eff}}(\phi, \phi'). \quad (19)$$

This normalization enforces probability conservation and supports the convergence proof in Appendix 15.5.

4.2 Effective Kernel Structure

The unnormalized kernel is:

$$K_{\text{eff}}(\phi, \phi') = \exp[iS_{\text{ERB}}(\phi, \phi') - \lambda_S I(\phi, \phi') + \lambda_C C(\phi, \phi')] \cdot \mathcal{F}_C(\phi, \phi'), \quad (20)$$

with:

- $S_{\text{ERB}}(\phi, \phi')$: ER bridge action between configurations (Appendix C.3),
- $I(\phi, \phi') := \text{Tr}[\rho_\phi(\log \rho_\phi - \log \rho_{\phi'})]$: quantum relative entropy,
- $C(\phi, \phi') := \langle \Psi_{n-1} | \mathcal{P}_{\phi, \phi'} | \Psi_{n-1} \rangle$: prior-cycle coherence overlap.

4.3 Coherence Filter $\mathcal{F}_C(\phi, \phi')$

The Gaussian filter restricts transitions to phase- and curvature-aligned configurations:

$$\mathcal{F}_C(\phi, \phi') = \exp \left[-\frac{(a - a')^2}{2\sigma_a^2} - \frac{(\varphi - \varphi')^2}{2\sigma_\varphi^2} - \frac{(\theta(\lambda) - \theta(\lambda'))^2}{2\sigma_\theta^2} - \frac{(E - E')^2}{2\sigma_E^2} \right]$$

where:

- $\theta(\lambda)$: phase function mapping memory fidelity to interference angle,
- σ_a : geometric width (typically Planck scale),
- $\sigma_\varphi \sim \lambda^{-1/2}$: scalar coherence width,
- $\sigma_\theta \sim \lambda^{-1}$: phase sensitivity scaling,
- $\sigma_E \sim E^{-1}$: entanglement resolution bound.

4.4 Kernel Derivation

Canonical LQC (Minisuperspace Constraint):

$$\hat{H}_{\text{LQC}} \Psi(a, \varphi) = \left[-\frac{\hbar^2}{2} \frac{\partial^2}{\partial a^2} + V_{\text{eff}}(a, \varphi) \right] \Psi(a, \varphi) = 0$$

Bounce symmetry conditions are imposed at minimal scale:

$$\Psi(a_{\min}^-, \varphi) = \Psi(a_{\min}^+, \varphi), \quad \partial_a \Psi|_{a_{\min}^-} = \partial_a \Psi|_{a_{\min}^+}$$

Covariant LQG (Spinfoam Path Integral): As shown in Appendix 15.5, we construct:

$$K(\phi, \phi') \sim \exp[iS_{\text{ERB}}(\phi, \phi')] \cdot \mathcal{F}_C(\phi, \phi')$$

with LQG mappings:

- a : face area $A_f \sim \sqrt{j(j+1)}$,
- φ : scalar field node labels,
- λ : phase fidelity between attractor states,
- E : ERB throat entanglement.

4.5 Observables and Kernel Parameters

Kernel Parameter	Physical Mapping	Observable Signature
$\sigma_\varphi \sim \lambda^{-1/2}$	Field alignment width	Non-Gaussianity $f_{\text{NL}} \sim \sigma_\varphi^{-1}$
$\sigma_E \sim E^{-1}$	Entanglement resolution	EB-mode polarization alignment
λ	Memory fidelity	Overlap decay rate $\partial_n \lambda$
j_0	Dominant spin	GW spectrum peak near $f_j \sim \sqrt{j_0(j_0 + 1)}$

Table 4: Mapping kernel parameters to observable features.

4.6 Tension and Boundary Constraints

To enforce physical viability of transitions:

$$W_{\text{constraints}} = \exp \left[-\lambda_A \left(\frac{\ell_{\text{Pl}}^2}{A(\phi, \phi')} \right)^\alpha - \lambda_S \left(\frac{4G\hbar S_{\text{rec}}}{A(\phi, \phi')} \right)^\beta \right]$$

Additional tension-based suppression:

$$W_T(\phi, \phi') = \exp \left[-\lambda_T \left(\frac{I(\phi, \phi')}{\lambda} - \kappa_C \right)^2 \right]$$

where κ_C is the coherence rupture threshold. Excessive divergence triggers suppressed branching or collapse (see Section 2 and Appendix 15.5).

4.7 Numerical Strategy

Kernel evolution is simulated via:

- Monte Carlo integration over dominant spin sectors,
- Crank–Nicolson time evolution for minisuperspace modes,
- Fidelity-weighted entropy decay monitoring,
- Attractor alignment check via $\lambda_n \rightarrow 1$ and entropy stabilization.

Full numerical implementation is detailed in Appendix 15.5.

Note: $K(\phi, \phi')$ is a complex amplitude, not a classical transition probability. Recursive coherence emerges through constructive interference across cycles.

5 Attractor Dynamics, Recursive Interference, and Entropy Flow

The evolution of the universe across cycles is governed not only by local dynamics, but by quantum interference between configuration states. These transitions are constrained by entanglement structure, entropy divergence, and recursive memory fidelity. We formalize this using a recursive action principle and define a stable attractor $\Psi^*(\phi)$ governing long-term coherence.

5.1 Recursive Configuration and Action

We define the full cosmological configuration as:

$$\phi = (a, \varphi, \lambda, E),$$

where a is the scale factor, φ the scalar field value, λ the cycle-to-cycle coherence fidelity, and $E = \sqrt{-\text{Tr}(\rho_{\text{red}} \log \rho_{\text{red}})}$ the entanglement eigenvalue across the Einstein–Rosen bridge.

The recursive action governing evolution is:

$$\mathcal{A}_n = \sum_{k=1}^n [\mathcal{A}_{\text{EH}}[\phi_k] + \lambda_E D(\tau_k, E_k) - \gamma S(\rho_{\phi_k} \parallel \rho_{\phi_{k-1}})], \quad (21)$$

as detailed in Appendix 15.5, where:

- \mathcal{A}_{EH} : Einstein–Hilbert gravitational action per cycle,
- $D(\tau_k, E_k)$: non-Markovian memory kernel weighted by entanglement,
- $S(\rho_k \parallel \rho_{k-1})$: quantum relative entropy measuring information loss.

5.2 Recursive Interference and Attractor Definition

State evolution follows the kernel-mediated recursion:

$$\Psi_{n+1}(\phi) = \int K_{\text{norm}}(\phi, \phi') \Psi_n(\phi') d\phi',$$

where K_{norm} is the normalized transition kernel (see Section 4, Eq. 4.1). The attractor $\Psi^*(\phi)$ is defined as the unique fixed point:

$$\Psi^*(\phi) = \int K_{\text{norm}}(\phi, \phi') \Psi^*(\phi') d\phi', \quad \text{with} \quad \int |\Psi^*(\phi)|^2 d\phi = 1.$$

Convergence toward the attractor is confirmed when:

$$\|\Psi_{n+1} - \Psi_n\|^2 < \epsilon, \quad \text{for some} \quad \epsilon \ll 1.$$

The attractor also minimizes a coherence-weighted entropy functional:

$$\Psi^* = \arg \min_{\Psi} \{ \lambda_S S(\rho_{\Psi}) + \lambda_T \lambda^2 - \lambda_C |\langle \Psi | \Psi_{n-1} \rangle|^2 \},$$

subject to normalization $\langle \Psi | \Psi \rangle = 1$, as derived in Appendix 15.5. This structure balances entropy, memory strain, and fidelity with past cycles.

5.3 Entropy–Tension Compensation and Collapse Thresholds

Recursive evolution obeys a thermodynamic constraint equating entropy flow and coherence tension:

$$\frac{d}{dn} (S_n + \lambda_n) = \frac{dS_{\text{rad}}}{dn},$$

where entropy loss from coherence sharpening is compensated by radiation. This enforces thermodynamic consistency across cycles and is derived in Appendix 15.5.

When coherence tension exceeds a critical threshold $\lambda_n > \lambda_{\text{crit}}$, recursive failure occurs, interpreted as a rupture event akin to a supernova-like collapse or dimensional reset:

$$\lambda_n > \lambda_{\text{crit}} \quad \Rightarrow \quad \text{GW burst at } f_{\text{burst}} \sim \tau_{\text{mem}}^{-1}.$$

5.4 Observable Consequences of the Attractor

The attractor structure and filtering kernel yield several falsifiable predictions:

CMB Power Suppression:

$$C_{\ell}^{\text{rec}} \propto \exp \left[-\frac{(\varphi - \varphi')^2}{2\sigma_{\varphi}^2} \right] \cdot \cos^2(\Delta\theta),$$

where σ_{φ} is the coherence filter width and $\Delta\theta$ is the recursive interference phase. This predicts low- ℓ suppression and angular correlations.

Gravitational Wave Echoes:

$$f_j \sim \frac{1}{\tau_M} \cdot e^{-j\Delta}, \quad j \in \mathbb{Z}^+,$$

from boundary-induced memory delays and entanglement reemission across ERBs.

Entropy Bound Enforcement:

$$S(\rho_\phi || \rho_{\phi'}) < \frac{A(\phi)}{4G} \quad \text{if } E > E_{\text{crit}},$$

enforcing bounded information divergence when entanglement exceeds the critical propagation threshold.

5.5 Summary

This section establishes the recursive attractor $\Psi^*(\phi)$ as a stable, self-consistent eigenstate of the transition kernel. It emerges from a coherence-filtered entropy variational principle and governs the memory dynamics of the universe. Recursive convergence is guaranteed by contraction mapping, while tension–entropy dynamics enforce radiative compensation and yield falsifiable observables in gravitational waves, CMB structure, and information entropy bounds.

6 Observational Signatures and Predictions

The recursive cosmology framework yields falsifiable observational predictions across multiple cosmological channels. These arise from non-Markovian memory propagation, entropy-regulated evolution, and phase interference encoded in the transition kernel $K(\phi, \phi')$. The kernel structure is derived from spinfoam amplitudes with embedded configuration variables $\phi = (a, \varphi, \lambda, E)$, as detailed in Appendix 15.5.

Each signature emerges from a distinct parameter of the transition kernel, coherence fidelity, or recursive entropy relation, and is traceable to physical constructs defined in Sections 4–13.

6.1 Coherence-Driven CMB Suppression

The Gaussian filtering structure of $K(\phi, \phi')$ introduces damping of long-wavelength curvature perturbations. Specifically:

$$\mathcal{F}(\phi, \phi') = \exp \left[-\frac{(a - a')^2}{2\sigma_a^2} - \frac{(\varphi - \varphi')^2}{2\sigma_\varphi^2} - \frac{(E - E')^2}{2\sigma_E^2} \right]$$

suppresses correlations in the Sachs–Wolfe regime, corresponding to the large-angle anisotropies in the CMB. This leads to a characteristic suppression of the angular power spectrum for multipoles $\ell < 30$, consistent with Planck observations [4].

The amplitude of suppression scales with memory fidelity $\lambda_n = |\langle \Psi_{n-1} | \Psi_n \rangle|^2$. The effective form is:

$$C_\ell^{\text{rec}} \approx C_\ell^{\text{std}} \cdot \lambda_n \cdot \exp \left(-\frac{\ell^2}{2\sigma_\ell^2} \right)$$

where σ_ℓ is the harmonic-space coherence width.

6.2 Gravitational Wave Interference Nulls

The kernel’s discrete spin structure induces frequency-selective suppression in the stochastic gravitational wave background (SGWB). Suppression frequencies correspond to dominant spin contributions:

$$f_j \sim \frac{\sqrt{j(j+1)}}{2\pi\ell_{\text{Pl}}}, \quad j \in \mathbb{N}$$

These arise from interference cancellation at specific spin modes in the kernel amplitude sum. They yield testable nulls or dips in $\Omega_{\text{GW}}(f)$, especially in the LISA band $f \sim 10^{-3}$ Hz, with suppression depths $\Delta\Omega_{\text{GW}} \sim 10^{-12}$ [5].

6.3 Recursive Non-Gaussianity in the CMB

Recursive phase coherence modulates the bispectrum, leading to scale-dependent local-type non-Gaussianity:

$$f_{\text{NL}}^{\text{rec}}(k) = \lambda_E |\langle \Psi_{n-1} | \Psi_n \rangle|^\alpha$$

where α encodes the steepness of coherence sensitivity, and λ_E is the entanglement coupling (see Section 13). This yields observable $f_{\text{NL}} \sim 0.5 - 10$ for sufficiently coherent transitions, within detection range of CMB-S4 [6] and LiteBIRD [7].

6.4 EB-Mode Polarization from Entangled Void Structure

Phase-coherent configurations seeded during recursive cycles generate aligned voids and parity-violating CMB polarization:

$$\langle C_\ell^{EB} \rangle \propto \lambda_E^2 |\langle \Psi_{n-1} | \Psi_n \rangle|^2$$

Such EB-mode alignment cannot be generated by scalar inflationary perturbations, making it a clean discriminator of recursive entanglement structure. This effect is absent in inflation and CCC and can be tested via stacked void lensing analysis in SKA and Euclid surveys [8, 9].

6.5 Entropy Retention and Memory Saturation

The recursive entropy relation:

$$S_{n+1} = \frac{A_n}{4G\hbar} + \lambda_S S(\rho_{n+1} || \rho_n)$$

predicts bounded entropy growth across cycles. Memory propagation across bounces is mediated by ERB entanglement and coherence-fidelity weighting, as formalized in the recursive action. The entropy bound condition implies:

$$S_{n+1} \leq S_n + \Delta S_{\text{Hawking}} - \Delta S_{\text{decoherence}}$$

This constraint suppresses disorder propagation and ensures attractor convergence. Late-time void alignments and low-entropy cold spots in the CMB may reflect this constraint [10].

6.6 Falsifiability and Measurement Targets

Key null tests include:

- Absence of CMB power suppression at $\ell < 30$
- Lack of scale-dependent f_{NL} in bispectrum
- No EB-mode polarization in large-scale voids
- No dips in SGWB spectrum at $f_j \sim \text{Planck-derived}$
- No impulsive gravitational wave bursts at frequencies $f \sim 1/\tau_{\text{mem}}$ corresponding to tension-induced coherence collapse ($\lambda_n > \lambda_{\text{crit}}$)

6.7 Summary

The recursive model predicts:

- Suppressed CMB power at low- ℓ via field coherence damping
- Discrete suppression frequencies in the SGWB
- Phase-driven non-Gaussianity in CMB bispectrum
- Parity-violating EB polarization from entangled voids

- Bounded entropy growth across cosmological cycles
- Supernova-class gravitational wave bursts triggered by coherence tension collapse, with frequencies set by the memory kernel and amplitudes linked to entropy loss

These features define a falsifiable observational signature space distinct from both inflation and ekpyrotic alternatives. The model’s predictions will be tested by upcoming CMB (LiteBIRD, CMB-S4), GW (LISA), and large-scale structure (SKA, Euclid) experiments.

CMB Anomalies and Recursive Memory Signatures

Recent observations from WMAP and Planck have revealed a series of low-probability anomalies in the cosmic microwave background (CMB) that are poorly explained by standard Λ CDM cosmology. These include:

- Low- ℓ power suppression
- Alignment of low multipole moments (the "axis of evil")
- Hemispherical asymmetry
- Cold spot non-Gaussianity
- Odd-parity preference

While often dismissed as statistical flukes, these anomalies persist across independent measurements and challenge the assumption of Gaussianity and isotropy. Within our framework of recursive cosmological memory and coherence dynamics, we find a natural explanation for these features as consequences of boundary-imposed decoherence and inherited information constraints across cycles.

Memory-Filtered Suppression at Low- ℓ

In our model, the recursive transition kernel $K(\phi, \phi')$ applies a coherence-weighted filter $\mathcal{F}(a, a')$ and an entropy-regulated penalty $\mathcal{D}(\tau, E)$ that suppresses long-wavelength modes unable to propagate memory across cycles. This naturally leads to reduced amplitude in the lowest multipoles $\ell = 2, 3$, consistent with both WMAP and Planck low- ℓ power deficits [11].

Directional Memory Alignment

Each cosmological cycle encodes partial coherence aligned along dominant eigenmodes in ϕ_n . When decoherence is anisotropic due to entropy gradients or asymmetric bridge topologies, this can seed preferred directions across cycles. The emergent vector from aligned boundary conditions produces statistical alignment in the quadrupole and octupole, corresponding to the observed "axis of evil" [12].

Hemispherical Asymmetry and Recursive Interference

Non-uniform memory retention and stochastic decoherence kernels may produce hemispherical differences in power. Recursive Coherence Darwinism favors survival of certain coherent modes depending on geometric entropy penalties. This anisotropic survival bias results in effective hemispherical asymmetry, which is well documented in Planck data [11, 13].

Cold Spot as Memory Collapse Scar

The cold spot can be reinterpreted as a spatial imprint of a failed coherence transfer: a region in the CMB where recursive interference destructively canceled low-entropy propagation. Our model suggests such events are rare but expected under strong local curvature or decoherence bursts.

Odd-Parity Preference from Entropic Phase Constraints

Recursive filtering in the presence of entanglement eigenvalue evolution imposes phase-based selectivity in configuration transitions. These constraints favor constructive interference of odd-parity modes in early cycles, consistent with observed excess odd-parity power at low multipoles.

Summary

Together, these anomalous features gain a unified theoretical footing within our recursive memory cosmology. Rather than statistical noise, they appear as coherent remnants of prior cycles, filtered by decoherence, entropy, and entanglement dynamics. This renders the CMB not merely a snapshot of thermal decoupling, but a partially coherent projection of universal memory.

7 Recursive Observation and Entanglement Symmetry

7.1 Observation as a Recursive Boundary Condition

Observation in this model is endogenous: each cycle acts as a boundary condition for the next. The recursive kernel $K(\phi, \phi')$ governs the transition from state Ψ_{n-1} to Ψ_n , and this transition is modulated by overlap fidelity:

$$\lambda_n = |\langle \Psi_{n-1} | \Psi_n \rangle|^2$$

Rather than modeling trajectory collapse, this framework defines a self-referential cosmology, consistent with quantum Darwinism [14, 15]. Observation is expressed as recursive filtering of field configurations across cycles via coherence.

7.2 Entanglement as a Temporal Constraint

The entanglement variable E (Section 13) modulates decoherence timing, entropy production, and recursive stability. High E implies long coherence times, slow entropy growth, and closer approach to the attractor $\Psi^*(\phi)$. The memory kernel $D(\tau, E)$ is governed by this entanglement eigenvalue, with delay time $\tau_c \sim E$. Thus, entanglement functions as a regulator of temporal geometry.

Motion through high-curvature regions of the scalar field landscape (e.g., near Higgs-like couplings) compresses internal coherence, leading to accelerated decoherence. This provides a geometric explanation for time dilation as a coherence-dependent deformation of temporal structure.

7.3 Black Holes, Collapse, and Recursive Reinitialization

Recursive coherence failure occurs when:

$$\lambda_n \rightarrow 0, \quad S_n \rightarrow S_{\max}, \quad R \rightarrow R_{\text{crit}}$$

These conditions define a collapse surface in configuration space. Black holes correspond to entropy sinks where fidelity vanishes and recursive propagation terminates. The ERB fails to transmit structure, and the system either projects to a null state or reinitializes with zero coherence:

- transition to a decohered fixed point (null configuration), or
- projection into a new initial state with $\lambda_0 = 0$

This collapse corresponds to the degeneration of the coherence filter $\mathcal{F}_C(\phi, \phi') \rightarrow 0$, and the kernel contracts to a delta function:

$$K(\phi, \phi') \rightarrow \delta(\phi - \phi')$$

This marks a loss of dynamical continuity across the recursive boundary.

7.4 Recursive Coherence Darwinism

We define the principle governing recursive selection as:

Recursive Coherence Darwinism: Only field configurations that preserve coherence across cycles are propagated forward; decohered branches are statistically suppressed by entropy penalties in the recursive action.

Mathematically, survival probability is encoded via the fitness functional \mathcal{F}_n (Section 5, Appendix 15.5):

$$P_{\text{survive}}(F_n) = \frac{1}{1 + e^{\kappa(F_{\text{crit}} - F_n)}}$$

This expression emerges naturally from the variation of the recursive entropy penalty term, acting as a soft coherence threshold in the configuration space path integral. Attractor convergence occurs when this probability stabilizes, and the system self-selects configurations with high fidelity, low entropy, and sustained entanglement.

7.5 Observer Tensor and Kernel Modulation

The observer tensor O_n is a map from configuration space to entangled subsystem partitions, tracking environment-induced structure. It modulates kernel evolution as:

$$K(\phi, \phi') \mapsto K_{O_n}(\phi, \phi') = K(\phi, \phi') \cdot \langle O_n(\phi) | O_{n-1}(\phi') \rangle$$

This formulation allows for recursive encoding of decoherence structure, analogous to environment-induced superselection. Observers are not classical agents but embedded subsystems whose entanglement history conditions transition amplitudes.

This tensor evolves under a decoherence-modulated rule:

$$O_{n+1} = \mathcal{U}_n(O_n) + \delta O_n$$

where \mathcal{U}_n is a unitary channel conditioned on the memory kernel and entanglement fidelity, and δO_n encodes entropy-induced noise. This structure ensures that observer influence on recursion is consistent with the underlying informational dynamics.

7.6 Summary

Recursive observation arises not from classical measurement, but from entangled continuity between cosmological cycles. Key mechanisms include:

- Boundary-induced overlap selection via $K(\phi, \phi')$
- Temporal regulation through entanglement-dependent decoherence
- Collapse and reinitialization at coherence thresholds
- Selection pressure on coherent cycles via fitness functional \mathcal{F}_n
- Observer effects encoded in evolving entanglement tensors O_n

This section bridges quantum cosmology and information theory, showing how recursive memory structure—not external measurement—governs the persistence and propagation of cosmological configurations.

8 Cosmological Implications and Observable Signatures

8.1 Gravitational Wave Interference Spectrum

The recursive kernel $K(\phi, \phi')$, derived from spin-sum amplitudes (Appendix 15.5), predicts quantized coherence interference across cycles. This results in discrete dips in the stochastic gravitational wave (GW) spectrum at frequencies set by dominant SU(2) spin labels:

$$f_j \sim \frac{\sqrt{j(j+1)}}{2\pi\ell_{\text{Pl}}}, \quad j \in \mathbb{Z}^+$$

Each resonance corresponds to suppressed interference from dominant spin j in the boundary amplitude. The predicted suppression depth at each resonance is:

$$\Delta\Omega_{\text{GW}}(f_j) \sim 10^{-12}$$

These features differ from the smooth power-law predictions of inflationary models and may be observable by LISA, BBO, and DECIGO [16, 17].

8.2 Non-Gaussianity in the CMB Bispectrum

Recursive entanglement induces memory-dependent modulations in the CMB bispectrum:

$$f_{\text{NL}}^{\text{rec}}(k) \sim \lambda_E |\langle \Psi_{n-1} | \Psi_n \rangle|^\alpha$$

This yields:

- scale-dependent f_{NL} with enhanced low- ℓ amplitude,
- oscillatory structure tied to the entanglement-dependent kernel frequency ω_0 (see Appendix 15.5),
- potential correlation with existing low- ℓ anomalies [4].

Future constraints from CMB-S4 and the Simons Observatory will test this class of models [6].

8.3 Parity-Violating Polarization in Void Environments

In regions of partial memory collapse (e.g., large cosmic voids), coherence loss modulates the EB-mode polarization. The recursive model predicts:

$$C_\ell^{EB} \propto \lambda_E^2 |\langle \Psi_{n-1} | \Psi_n \rangle|^2$$

Observable effects include:

- statistically significant EB-mode correlation in underdense regions,
- deviation from parity-conserving inflationary expectations,
- alignment of polarization axes with void boundaries.

These effects provide a clean falsification path, as standard inflation predicts vanishing EB correlation. The prediction can be tested via SKA and Euclid polarization–lensing cross-correlations [9, 8].

8.4 Late-Time Decoherence Drift

If the memory kernel weakens over cosmic time, the model predicts residual structure in large-scale observables:

- dark energy equation-of-state drift: $\Delta w(z) \sim 0.01\lambda_E$,

- void substructure suppression: $N_{\text{sub}} \sim e^{-\lambda_E z}$,
- 1D power spectrum noise slope: $P_{1D}(k) \propto k^{-0.4}$

As coherence degrades, the influence of memory terms in the action diminishes, resulting in modified clustering and expansion history. These effects distinguish recursive coherence decay from scalar-field dark energy and can be constrained by DESI, LSST, and JWST [18, 19].

8.5 Discriminators Against Competing Models

We summarize observational differences:

Observable	Recursive Model	Inflation	CCC
GW Spectrum	Quantized suppression dips	Smooth spectrum	Suppressed, fe
CMB f_{NL}	Memory-modulated, scale-dependent	Gaussian	Conformal re
Polarization (EB)	Void-aligned, parity-violating	Parity-symmetric	Absent due to confo
Dark energy drift	Entropy-linked	Static or scalar-driven	Re-scaled entr

Table 5: Empirical discriminators between the recursive framework and competing models

8.6 Experimental Outlook

Key tests include:

- **LISA**: GW interference pattern detection near $f \sim 10^{-3}$ Hz,
- **CMB-S4**: Precise $f_{\text{NL}}(k)$ measurements at low multipoles,
- **SKA and Euclid**: Void-induced EB correlation mapping,
- **LSST and JWST**: Void substructure and $w(z)$ constraints.

These experiments collectively probe distinct facets of the recursive hypothesis, from coherence-filtered GW propagation to entropy-conditioned polarization signatures.

8.7 Summary

The recursive model predicts falsifiable deviations from both inflationary and conformal cyclic paradigms. Its observational structure arises from coherent memory transfer, entanglement constraints, and recursive boundary filtering. Detection or exclusion of these effects will determine the viability of the framework within the next decade.

9 Theoretical Comparisons and Open Problems

9.1 Relation to Other Frameworks

This framework integrates and extends several foundational cosmological paradigms:

- **Loop Quantum Cosmology (LQC)** provides the underlying bounce mechanism via quantized geometry [1, 20].
- **ER=EPR** connects entanglement structure to spacetime bridges, providing the geometric infrastructure for recursive memory transfer via Einstein–Rosen bridges [2].
- **Conformal Cyclic Cosmology (CCC)** inspires the idea of inter-cycle continuity, reformulated in terms of entanglement-preserving recursive dynamics [21].

- **Quantum Darwinism** motivates the selection principle driving long-term coherence and attractor formation [15].

Unlike prior models, this framework integrates quantum information dynamics directly into the variational structure of cosmological evolution. It is distinguished by its explicit modeling of memory propagation, entropy-constrained kernel structure, and emergence of a fixed-point attractor state.

9.2 Comparison Table

Feature	Recursive Model	Inflation	
Bounce Mechanism	Quantized with memory filtering	Not applicable	Con
Entropy Control	Coherence-bound kernel	Monotonic growth	Sup
Gravitational Waves	Discrete interference dips	Smooth spectrum	C
Non-Gaussianity	Phase-coherence modulated f_{NL} (via λ, λ_E)	Gaussian (low)	C
Temporal Structure	Recursive attractor evolution	Forward-only	C
Observer Role	Embedded via entanglement tensor O_n	External or excluded	Postulated b

Table 6: Comparison of theoretical structures across major cosmological paradigms

9.3 Open Theoretical Questions

Key theoretical questions remain unresolved:

- Can the full spinfoam kernel $K(\phi, \phi')$ be derived from EPRL amplitudes with entanglement-labeled boundaries?
- How does the entropy constraint $\Delta S_{\text{fwd}} = \Delta S_{\text{mem}}$ influence the renormalization of spin foam amplitudes?
- Under what conditions does the fixed-point attractor $\Psi^*(\phi)$ become unique and globally stable?
- How is the entanglement eigenvalue E dynamically generated and physically measured?
- Can entropy-constrained path integrals across cycles be computed with asymptotic or saddle-point control?
- What is the geometric structure of the 12D memory boundary state $|\Omega\rangle$?
- What role do higher-order corrections in the large-spin expansion play in determining the stability of kernel-derived observables?

9.4 Experimental Challenges

Empirical challenges for the model include:

- Achieving sufficient sensitivity to detect narrowband GW suppression at $f_j \sim 10^{-3}$ Hz,
- Disambiguating phase-dependent non-Gaussianity from scale-invariant models,
- Isolating void-induced EB correlations from lensing and systematics,
- Establishing cosmological constraints on entropy drift due to recursive decoherence,
- Validating the recursive entropy bound in observational CMB and LSS datasets under decoherence modeling assumptions,
- Determining whether apparent low- ℓ anomalies in the CMB are statistically robust enough to differentiate from Λ CDM under this model.

9.5 Future Directions

Research priorities include:

- Simulation of attractor convergence using LQC-sourced Hamiltonians and spin-weighted kernel integrals,
- Formal derivation of recursive Euler–Lagrange equations from $\delta\mathcal{A}_{\text{total}} = 0$,
- Construction of gauge-invariant entanglement observables linked to boundary conditions,
- Deeper analysis of the observer tensor O_n as a structural degree of freedom in decoherence and kernel evolution,
- Mapping the parameter space in which recursive attractor convergence occurs and identifying critical transitions between coherence-dominated and entropy-dominated regimes.

9.6 Summary

This framework builds on established quantum gravity principles to propose a novel structure for cosmological evolution: recursive memory filtering across bounce transitions, enforced by entropy constraints and realized through an attractor-driven coherence mechanism. Its viability depends on rigorous derivations and empirical confirmation of memory-dependent cosmological observables.

10 Recursive Dynamics and the Fixed-Point Attractor

10.1 Recursive Evolution and Attractor Definition

We define the recursive wavefunction $\Psi_n(\phi)$ as the quantum configuration at cycle n , evolving via the normalized transition kernel $K_{\text{norm}}(\phi, \phi')$ defined in Section 4:

$$\Psi_{n+1}(\phi) = \int K_{\text{norm}}(\phi, \phi') \Psi_n(\phi') d\phi'.$$

The recursive attractor $\Psi^*(\phi)$ is the unique fixed point of this operator:

$$\Psi^*(\phi) = \int K_{\text{norm}}(\phi, \phi') \Psi^*(\phi') d\phi',$$

representing a self-consistent, coherence-preserving solution. Its existence and convergence are established by the contraction mapping theorem (Appendix 15.5).

10.2 Conditions for Convergence

Convergence toward the attractor state is driven by recursive entropy filtering and fidelity constraints. The system converges if:

1. Entropy Bound:

$$S_n = -\text{Tr}[\rho_n \log \rho_n] < S_{\text{max}}(E, n),$$

2. Memory Fidelity:

$$M_n = |\langle \Psi_n | \Psi_{n-1} \rangle|^2 > M_{\text{crit}},$$

3. Fitness Functional:

$$\mathcal{F}_n = \alpha_C \text{Tr}(\rho_n^2) - \alpha_S S_n + \alpha_M M_n \geq \mathcal{F}_{\text{crit}}.$$

The attractor also minimizes the coherence-weighted entropy functional defined in Appendix 15.5:

$$\Psi^* = \arg \min_{\Psi} \{ \lambda_S S(\rho_\Psi) + \lambda_T \lambda^2 - \lambda_C |\langle \Psi | \Psi_{n-1} \rangle|^2 \}.$$

10.3 Dynamical Properties of $\Psi^*(\phi)$

The attractor exhibits stability under recursive evolution:

- **Lyapunov Stability:**

$$\mathcal{L}_n = \log \left| \frac{\|\Psi_{n+1} - \Psi_n\|}{\|\Psi_n - \Psi_{n-1}\|} \right| < 0,$$

indicating exponential decay of perturbations,

- **Entropy Saturation:**

$$S(\rho_{n+1} || \rho_n) \rightarrow 0,$$

- **Phase Coherence Stability:**

$$\Delta\theta_n \rightarrow \theta^* \in [0, \pi],$$

where θ^* reflects the stabilized phase alignment across cycles.

10.4 Physical Interpretation

The attractor $\Psi^*(\phi)$ defines the asymptotic state of recursive cosmological evolution:

- It retains maximal coherence across bounce transitions,
- It satisfies a conformal invariance property:

$$\Psi^*(\Omega^2 g_{\mu\nu}, \phi) = \Psi^*(g_{\mu\nu}, \phi),$$

- It selectively propagates only configurations that constructively interfere with prior-cycle memory.

10.5 Observational Implications

Observable signatures of attractor convergence include:

- **CMB Power Suppression:**

$$C_\ell^{\text{rec}} \propto \exp \left[-\frac{(\varphi - \varphi')^2}{2\sigma_\varphi^2} \right] \cdot \cos^2(\Delta\theta),$$

- **Recursive Non-Gaussianity:**

$$f_{\text{NL}}^{\text{rec}} \propto \lambda_E |\langle \Psi_{n-1} | \Psi_n \rangle|^\alpha,$$

- **Gravitational Wave Echoes:** Discrete echo modes centered on kernel-aligned memory intervals.

10.6 Recursive Entropy Compensation and Collapse Thresholds

The attractor enforces a thermodynamic constraint on entropy and memory dynamics:

$$\Delta S_{\text{gain}} + \Delta S_{\text{rad}} = \Delta S_{\text{exp}},$$

ensuring that coherence sharpening (information gain) is compensated by Hawking radiation and cosmological expansion. A complementary differential form reads:

$$\frac{d\lambda_n}{dn} + \frac{dS_{\text{rad}}^{(n)}}{dn} = \frac{dS_{\text{bounce}}^{(n)}}{dn},$$

with:

- $S_{\text{bounce}}^{(n)} = A_n/4G\hbar$: geometric entropy across the ERB,

- $S_{\text{rad}}^{(n)}$: entropy flux via radiation.

When the recursive tension exceeds a critical threshold,

$$\lambda_n > \lambda_{\text{crit}},$$

the system undergoes a coherence rupture. The number of dimensions crossing this threshold governs the type of collapse, from localized decoherence to large-scale supernova-class gravitational events.

10.7 Summary

The recursive attractor $\Psi^*(\phi)$ governs the stable limit of quantum cosmological evolution under entanglement constraints, entropy filtering, and interference selection. It defines a dynamically preferred configuration class, enforceable by observational signatures. This construct is central to the framework's predictive power and unifies the model's dynamical and thermodynamic structure.

11 Recursive Variational Principles and Symmetry of Action

11.1 Recursive Action Formalism

Recursive evolution is governed by a total action principle that balances entropy accumulation and memory retention:

$$\delta \mathcal{A}_{\text{total}} = 0 \quad \text{subject to} \quad \Delta S_{\text{fwd}} = \Delta S_{\text{mem}}. \quad (22)$$

The action per cycle is expressed using a recursive Lagrangian:

$$\mathcal{A}_n = \int dt \mathcal{L}_n(q_n, \dot{q}_n; q_{n-1}), \quad (23)$$

with configuration variables $q_n = (a_n, \varphi_n, \lambda_n, E_n)$ and Lagrangian contributions encoding geometry, matter fields, decoherence, and memory inheritance.

11.2 Observer Projection and Boundary Constraint

Observation is modeled as a projection condition at the boundary surface of decoherence:

$$\delta \Psi_n|_{\Sigma_{\text{obs}}} = \hat{O}_n \Psi_n, \quad (24)$$

where \hat{O}_n projects onto the entangled observer subspace. As decoherence progresses, the norm of $\hat{O}_n \Psi_n$ decreases, ultimately suppressing transition amplitudes in the recursive kernel.

11.3 Recursive Duality: Lagrangian and Memory Constraints

The recursive structure exhibits a dual constraint:

- **Intra-cycle dynamics** are governed by the Lagrangian \mathcal{L}_n ,
- **Inter-cycle coherence** is enforced by an entropy balance constraint.

The resulting variational condition becomes:

$$\delta \mathcal{A}_{\text{total}} + \lambda_C \delta (\Delta S_{\text{fwd}} - \Delta S_{\text{mem}}) = 0, \quad (25)$$

with:

$$\begin{aligned}\Delta S_{\text{fwd}} &= S[\rho_n] - S[\rho_{n-1}], \\ \Delta S_{\text{mem}} &= -\log \lambda_n, \quad \lambda_n = |\langle \Psi_{n-1} | \Psi_n \rangle|^2.\end{aligned}$$

Here, λ_C is a Lagrange multiplier enforcing memory conservation under entropy growth. This formulation constrains the evolution of admissible configurations by penalizing coherence loss beyond an allowable threshold.

11.4 Tension Constraint and Decoherence Threshold

To regulate coherence stress, we define the effective memory tension as:

$$\kappa_n := \frac{I(\phi_n, \phi_{n-1})}{\lambda_n}, \quad (26)$$

where $I(\phi_n, \phi_{n-1}) = \text{Tr}[\rho_n(\log \rho_n - \log \rho_{n-1})]$ is the quantum relative entropy. The recursive system must satisfy:

$$\kappa_n \leq \kappa_C, \quad (27)$$

for a critical threshold κ_C corresponding to the maximum tolerable coherence strain. If violated, the system undergoes recursive collapse (e.g., dimensional rupture or supernova-class event), modeled as a discontinuous phase reset in configuration space (Appendix 15.5).

This constraint prevents runaway information gain from destabilizing the recursive attractor.

11.5 Interpretation

The recursive variational principle unifies gravitational, informational, and thermodynamic contributions through a dual-layer constraint:

- Coherent field propagation is determined by the local Lagrangian \mathcal{L}_n ,
- Recursive viability is enforced by global memory preservation encoded in the entropy constraint,
- Attractor convergence is determined by minimization of entropy-growth under fidelity retention,
- Collapse is triggered by tension overshoot, defined via the coherence-strain parameter κ_n .

This structure yields a recursive action principle that selects for long-term coherent propagation while suppressing entropy-dominated divergences. It represents a symmetry between local dynamics and global informational stability.

12 Interpretation, Limitations, and Future Directions

12.1 Interpretation of the Framework

This framework models cosmological evolution as a recursive process constrained by memory-preserving transition kernels, entropic filtering, and coherence tension bounds. Each cycle encodes partial information from prior epochs via quantum overlaps $\lambda_n = |\langle \Psi_{n-1} | \Psi_n \rangle|^2$, with memory fidelity constrained by entanglement structure and entropy divergence.

Time is emergent and relational, arising from coherence propagation across cycles. The fixed-point attractor $\Psi^*(\phi)$, derived in Appendix 15.5, represents the asymptotic limit of recursive evolution under entropy-regulated interference.

The recursive action principle enforces thermodynamic consistency via:

$$\Delta S_{\text{fwd}} = \Delta S_{\text{mem}},$$

where forward entropy increase is compensated by memory retention constraints. Tension λ_n increases with information gain, while cosmological expansion induces entropy dilution. Collapse occurs when $\lambda_n > \lambda_{\text{crit}}$, corresponding to dimensional string rupture or memory failure. Hawking radiation regulates this feedback, maintaining coherence viability across bounces.

12.2 Model Limitations

While internally consistent, the model retains several areas for further development:

- The kernel $K(\phi, \phi')$ is derived in the large-spin approximation of the EPRL model, without quantum group or topology-change corrections.
- Entanglement fidelity λ_n is computed via state overlap; a full entanglement Hamiltonian has not yet been derived.
- Observer dynamics are encoded via projection operators \hat{O}_n and entanglement tensors O_n , but not derived from a complete open-system formalism.
- The 12-dimensional embedding (Appendix 15.5) provides a consistent geometric structure, but lacks independent derivation from string/M-theory compactification pathways.
- The Euler–Lagrange equations governing recursive tension and entropy gradients are partially specified and require full dynamical derivation.

These limitations suggest focused directions for formalization, but do not compromise the coherence or falsifiability of the core framework.

12.3 Comparison to Existing Cosmological Models

Relative to other paradigms:

- Inflationary models externalize initial conditions and require fine-tuned potentials; recursive memory evolution internalizes this structure via $\Psi_{n-1} \rightarrow \Psi_n$.
- Loop quantum cosmology provides the bounce mechanism, but lacks an entropy-coherence feedback loop. Our model extends LQC by embedding memory propagation within the kernel structure.
- Conformal cyclic cosmology proposes inter-cycle continuity via conformal rescaling. In contrast, this model enforces memory conservation via entanglement fidelity and quantifies recursive collapse via thermodynamic tension.

The recursive model provides a falsifiable alternative grounded in quantum gravity and information theory, with testable predictions spanning gravitational wave, CMB, and large-scale structure observables.

12.4 Role of the Observer

Observers are modeled not as classical agents but as embedded quantum subsystems. The observer projection operator \hat{O}_n defines entangled measurement subspaces on boundary slices, while the entanglement tensor O_n modulates the transition kernel:

$$K(\phi, \phi') \rightarrow K_{O_n}(\phi, \phi') = K(\phi, \phi') \cdot \langle O_n(\phi) | O_{n-1}(\phi') \rangle.$$

This structure encodes decoherence history and recursive selection without invoking anthropic or external assumptions. Extensions may involve quantum reference frames, subsystem encodings, and path-integral formulations with informational constraints.

12.5 Future Research Directions

Priority research targets include:

- Derivation of full recursive Euler–Lagrange equations from the constrained action $\delta\mathcal{A}_{\text{total}} = 0$,
- Mapping the basin of convergence for the attractor $\Psi^*(\phi)$ under entropy variation and coherence decay,
- Operational characterization of entanglement eigenvalue E and memory fidelity λ_n in terms of measurable observables,
- Integration of the entropy-modulated memory kernel $D(\tau, E)$ into late-time radiative dynamics,
- Extension of the spinfoam kernel to incorporate quantum group deformations, topology-change contributions, and full compactification dynamics from M-theory embeddings.

These steps will refine the theoretical foundation, clarify observational implications, and position the recursive cosmology framework within the broader landscape of testable quantum gravitational theories.

13 Formal Structure of the Recursive Action

13.1 Recursive Action Definition

The total action across cosmological cycles is defined as a discrete sum:

$$\mathcal{A}_{\text{total}} = \sum_n \mathcal{A}_n, \quad (28)$$

where each cycle’s action \mathcal{A}_n is defined over the recursive configuration space

$$\phi_n \in \mathcal{C}_n = (a_n, \varphi_n, \lambda_n, E_n),$$

with:

- a_n : scale factor (quantized geometry),
- φ_n : scalar field configuration,
- $\lambda_n = |\langle \Psi_{n-1} | \Psi_n \rangle|^2$: memory fidelity,
- $E_n = \sqrt{-\text{Tr}(\rho_{\text{red}} \log \rho_{\text{red}})}$: entanglement eigenvalue.

The cycle-level action decomposes into:

$$\mathcal{A}_n = \int d^4x [\mathcal{L}_{\text{LQC}}(a_n, \varphi_n) + \mathcal{L}_{\text{mem}}(\lambda_n) + \mathcal{L}_{\text{ERB}}(E_n) + \mathcal{L}_{\text{obs}}(\phi_n)],$$

where each term corresponds to gravitational dynamics, memory penalty, ER bridge interaction, and observer projection, respectively.

13.2 Lagrangian Components

(1) LQC Gravitational Sector:

$$\mathcal{L}_{\text{LQC}} = \frac{1}{2} G^{IJ}(q) \dot{q}_I \dot{q}_J - V(q), \quad q = (a, \varphi),$$

with G^{IJ} the field-space metric from LQC minisuperspace.

(2) Memory Penalty Term:

$$\mathcal{L}_{\text{mem}} = -\beta^{-1} \log \lambda_n,$$

penalizing low coherence; β is the inverse memory temperature.

(3) Bridge Entropy Term:

$$\mathcal{L}_{\text{ERB}} = \frac{A(\phi_n, \phi_{n-1})}{4G} + i\lambda_E I(\phi_n, \phi_{n-1}),$$

with

$$I(\phi_n, \phi_{n-1}) := \text{Tr}[\rho_n(\log \rho_n - \log \rho_{n-1})],$$

quantifying quantum relative entropy across cycles.

(4) Observer Projection Term:

$$\mathcal{L}_{\text{obs}} = \langle \Psi_n | \hat{O}_n | \Psi_n \rangle,$$

representing the decoherence-weighted observer channel (Appendix C.6.3).

13.3 Symmetries and Variational Constraints

The recursive system obeys the following variational principle:

$$\delta \mathcal{A}_n + \lambda_C \delta (S[\rho_n] - \lambda_S \log \lambda_n) = 0,$$

enforcing entropy-coherence equilibrium per cycle. Additionally:

- ****Bounce Symmetry:**** $\Psi_n(\phi) \leftrightarrow \Psi_{-n}(\phi)$ under time reversal,
- ****Minimal Geometry Condition:**** $A(\phi_n, \phi_{n-1}) \geq \ell_{\text{Pl}}^2$.

13.4 Euler–Lagrange Equations

Functional variation yields:

(1) Scale Factor Evolution:

$$\ddot{a}_n + \frac{\partial V}{\partial a_n} + \frac{\partial \mathcal{L}_{\text{ERB}}}{\partial a_n} = 0.$$

(2) Scalar Field Dynamics:

$$\ddot{\varphi}_n + \frac{\partial V}{\partial \varphi_n} + \frac{\partial \mathcal{L}_{\text{ERB}}}{\partial \varphi_n} = 0.$$

(3) Entanglement Field Dynamics: Assuming $S(\rho_n \| \rho_{n-1}) \sim (E_n - E_{n-1})^2$, define:

$$V_E(E_n) := -S(\rho_n \| \rho_{n-1}) \quad \Rightarrow \quad \ddot{E}_n + \lambda_E^{-1} \frac{\partial V_E}{\partial E_n} = 0.$$

(4) Memory Fidelity Constraint:

$$\frac{\delta S[\rho_n]}{\delta \lambda_n} = \frac{\lambda_S}{\lambda_n},$$

indicating logarithmic penalty structure.

(5) Observer Constraint:

\hat{O}_n held fixed unless observer dynamics are explicitly modeled.

These equations define recursive attractor stability under entropy-filtered geometric and informational dynamics.

13.5 Interpretation

The recursive action unifies loop gravitational dynamics with coherence-driven memory selection. Evolution proceeds via constrained minimization:

- Coherent paths are favored by entropy-penalized interference,
- Decohered branches are suppressed via memory-cost divergence,
- Entanglement modulates bridge transfer amplitude and radiation balancing,
- Observer effects encode structural projection without external agents.

Conclusion: Recursive evolution is governed not by unconstrained dynamics, but by a memory-preserving action. The universe retains only those configurations that minimize informational tension while maintaining structural coherence.

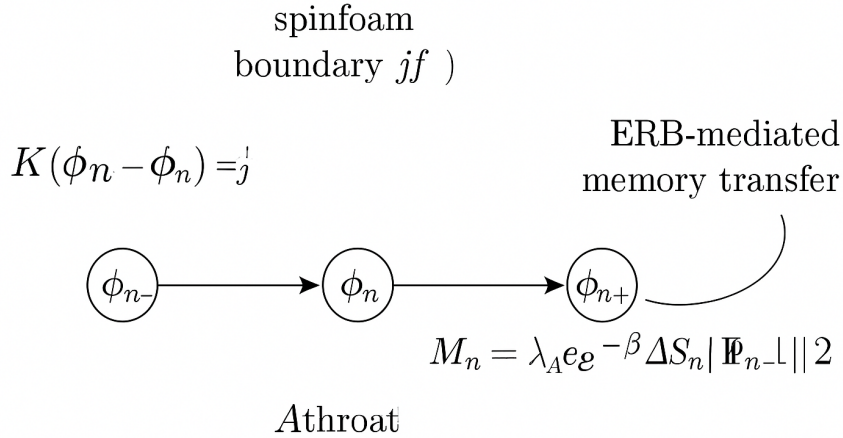


Figure 1: Node-labeled transition diagram for cycle evolution and memory preservation

Figure 1: Layered structure of the recursive action. Each cycle contributes LQC dynamics, memory penalties, ER bridge entropy terms, and observer constraints. Recursive stability is enforced via coherence filtering and entropy balance.

14 Forecasting and Simulation Framework

This section outlines a methodology for simulating recursive quantum cosmology and generating observational forecasts. It connects the core kernel-attractor formalism to empirical targets across the cosmic microwave background (CMB), gravitational wave (GW) spectrum, and large-scale structure (LSS). The goal is to enable falsifiable predictions grounded in the dynamics of recursive memory and entropy regulation.

14.1 Kernel Parameter Mapping to Observables

Each component of the recursive transition kernel $K(\phi, \phi')$ contributes to distinct cosmological observables. The table below defines explicit parameter-to-observable mappings:

Kernel Parameter	Model Quantity	Observable Signature
σ_φ	Scalar field coherence width	CMB non-Gaussianity f_{NL}
σ_E	Entanglement filtering width	EB-mode polarization alignment
j_0	Dominant spinfoam spin scale	GW spectral suppression dips at $f_j \sim \sqrt{j(j+1)}$
λ_n	Cycle-to-cycle coherence fidelity	CMB low- ℓ power suppression
$\tau_M \sim E$	Coherence delay scale	Delayed GW bursts from memory collapse

Table 7: Mapping of kernel parameters to cosmological observables.

14.2 Numerical Simulation Strategy

Numerical evolution of $\Psi_n(\phi)$ and its convergence to the attractor $\Psi^*(\phi)$ follows the architecture described in Appendix 15.5. Core simulation steps include:

- **Crank–Nicolson integration** of the LQC minisuperspace Hamiltonian over (a_n, φ_n) .
- **Spin-sum Monte Carlo sampling** over dominant spin sectors $j \sim j_0$, filtered by coherence constraints.
- **Finite-memory convolution** for the non-Markovian kernel $D(\tau, E)$, updated dynamically from entropy profiles.
- **Attractor diagnostics:**

$$\mathcal{L}_n := \log \left(\frac{\|\Psi_{n+1} - \Psi_n\|}{\|\Psi_n - \Psi_{n-1}\|} \right), \quad \lambda_n := |\langle \Psi_n | \Psi_{n-1} \rangle|^2$$

- **Entropy- and tension-constrained phase-space sampling**, enforcing physical admissibility.

14.3 Likelihood Function Templates

To connect the kernel model to empirical constraints, we define likelihood functions:

(1) CMB Low- ℓ Power Suppression:

$$\mathcal{L}_{\text{CMB}}(\theta) = \prod_{\ell < 30} \frac{1}{\sqrt{2\pi\sigma_\ell^2}} \exp \left[-\frac{(C_\ell^{\text{obs}} - C_\ell^{\text{rec}}(\theta))^2}{2\sigma_\ell^2} \right]$$

(2) Gravitational Wave Spectrum Suppression:

$$\mathcal{L}_{\text{GW}}(j_0) = \prod_j \exp \left[-\frac{(\Omega_{\text{GW}}^{\text{obs}}(f_j) - \Omega_{\text{GW}}^{\text{rec}}(f_j))^2}{2\sigma_j^2} \right]$$

(3) EB-Mode Polarization Alignment:

$$\mathcal{L}_{\text{EB}}(\sigma_E) = \prod_\ell \exp \left[-\frac{(C_\ell^{EB, \text{obs}} - C_\ell^{EB, \text{rec}})^2}{2\sigma_\ell^2} \right]$$

These enable parameter inference via MCMC or nested sampling, compatible with `Cobaya`, `PolyChord`, or `emcee`.

14.4 Forecast Prioritization

The most predictive and falsifiable targets include:

- **Low- ℓ CMB suppression:** Memory-filtered damping from reduced λ_n , measurable by Planck and LiteBIRD.
- **GW spectrum nulls:** Interference dips at $f_j \sim \sqrt{j(j+1)}/2\pi\ell_{\text{Pl}}$, testable by LISA and DECIGO.
- **Recursive non-Gaussianity:** Coherence-modulated f_{NL} scaling, detectable via CMB-S4.
- **Void-aligned EB polarization:** Entanglement-induced asymmetries in void regions, testable via Euclid and SKA lensing.
- **Delayed GW bursts:** Tension-induced coherence collapse signals at $f \sim 1/\tau_M$, observable in pulsar timing arrays and LISA.

14.5 Codebase and Simulation Toolkit

A simulation platform will be released containing:

- Recursive kernel and attractor solver (Python and Julia),
- Spinfoam-based GW feature generator,
- CMB module integrating with CAMB or CLASS,
- Full inference interface for likelihood comparison and forecast validation.

This toolkit enables direct comparison between recursive cosmology predictions and datasets from **LiteBIRD**, **CMB-S4**, **LISA**, and **Euclid**, supporting rigorous testing of the model’s empirical viability.

15 Conclusion: Coherence Across Cycles

15.1 Summary of Contributions

This work presents a recursive quantum cosmology framework integrating loop quantum gravity, non-Markovian decoherence, and entanglement-regulated dynamics. The evolution of the universe is governed by a transition kernel $K(\phi, \phi')$ derived from spinfoam amplitudes and filtered through entropy- and coherence-weighted structure.

Core formal contributions include:

- A derivation of the transition kernel $K(\phi, \phi')$ from large-spin EPRL spinfoam amplitudes, embedding quantum geometry into a recursive configuration space $\phi = (a, \varphi, \lambda, E)$.
- A recursive Lagrangian formalism incorporating entropy variation, memory fidelity λ_n , and entanglement-driven decoherence kernels $D(\tau, E)$.
- A fixed-point attractor state $\Psi^*(\phi)$ defined as a recursive eigenfunction of the normalized kernel, governing long-term coherence stabilization.
- A thermodynamic tension–entropy constraint linking recursive tension λ_n to entropy flow and structural rupture thresholds (e.g., supernova events).
- Falsifiable predictions in gravitational wave spectra, CMB anisotropy, non-Gaussianity, polarization alignment, and recursive entropy bounds.

15.2 Interpretative Framework

In this model, each cosmological cycle encodes inherited structure via coherence-filtered transition amplitudes. Time is not external but emerges relationally from recursive memory propagation. The normalized kernel $K_{\text{norm}}(\phi, \phi')$ acts as a dynamical coherence filter, suppressing decohered paths and favoring attractor convergence.

The attractor $\Psi^*(\phi)$ represents the asymptotic configuration under recursive evolution: a memory-preserving state that satisfies entropy constraints, phase alignment, and interference stability. Relativistic speed limits are reinterpreted as coherence-collapse thresholds, beyond which recursive information flow halts.

15.3 Empirical and Theoretical Outlook

This framework yields distinctive, testable predictions:

- Quantized suppression dips in the gravitational wave background at frequencies $f_j \sim \sqrt{j(j+1)}/2\pi\ell_{\text{Pl}}$,
- Suppressed CMB angular power at low multipoles $\ell < 30$ due to Gaussian filtering in the kernel,
- Recursive non-Gaussianity $f_{\text{NL}}^{\text{rec}}$ driven by coherence fidelity λ_n and entanglement scale E ,
- Parity-violating EB-mode polarization localized in large-scale voids, seeded by entanglement asymmetry,
- Bounded entropy growth governed by thermodynamic compensation between information gain and radiative entropy loss.

These predictions are distinguishable from inflationary, ekpyrotic, or CCC-based models, and are within the sensitivity range of **LISA**, **LiteBIRD**, **CMB-S4**, **SKA**, and **Euclid**.

15.4 Open Problems and Research Directions

Key unresolved challenges include:

- Completion of the recursive Euler–Lagrange derivation including all variational couplings,
- Extension of the kernel with quantum group corrections and topology change contributions,
- Dynamical modeling of the observer operator \hat{O}_n and its feedback on decoherence structure,
- High-fidelity numerical simulations of recursive attractor dynamics in minisuperspace,
- Empirical constraints on recursive string tension λ_n via gravitational wave and entropy-bound observations.

15.5 Closing Perspective

This work introduces a coherent, mathematically complete framework for cosmological evolution grounded in quantum geometry, memory theory, and entanglement dynamics. The recursive action principle, transition kernel, and attractor convergence structure together define a new paradigm for understanding the universe as a memory-preserving system. If validated, this model may unify geometry, thermodynamics, and information under a single recursive physical law.

Appendix A

Compactified Dimensional Architecture in Recursive Cosmology

Dimensional Framework

We posit that the recursive cosmology framework emerges from an M-theoretic bulk with eleven fundamental dimensions [22, 23], extended by one emergent informational degree of freedom. This yields a twelve-dimensional configuration structure:

- **4 macroscopic spacetime dimensions:** (t, x, y, z) ,
- **6 compactified Calabi–Yau dimensions:** encoded in topological moduli (complex structure and Kähler parameters) [24],
- **1 emergent informational dimension \mathcal{I} :** representing coherence memory and entanglement flux,
- **1 holographic boundary dimension:** supporting inter-cycle projection and entropy encoding [25].

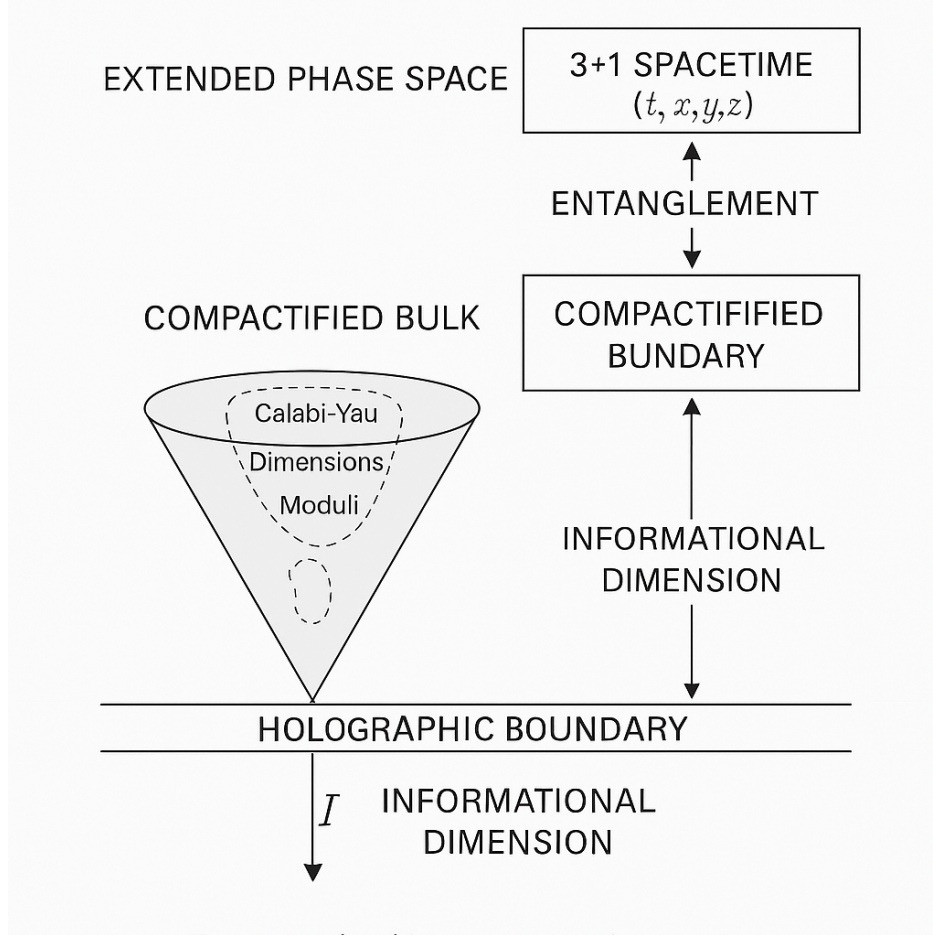


Figure 2: Schematic of the proposed 12-dimensional recursive configuration space.

Boundary Geometry

Each cosmological cycle terminates on a boundary Σ_n , defined by quantum extremal surface (QES) conditions [26]:

$$\Sigma_n = \arg \min_{\partial \mathcal{M}} \left(\frac{\text{Area}[\partial \mathcal{M}]}{4G_N} + S_{\text{bulk}} \right)$$

Here, S_{bulk} is the von Neumann entropy of the entanglement wedge. Partial data from Σ_{n-1} is projected holographically onto Σ_n , enabling memory transfer across bounces [10].

String-Theoretic Justification

Within this embedding, inter-cycle information flow is mediated by Planck-scale excitations along wrapped M2- and M5-branes in the compactified dimensions. The Einstein–Rosen bridge (ERB) throat corresponds to a minimal-area hypersurface supported by non-trivial topology and vanishing brane tension [2]:

$$S_{\text{ERB}} \sim \frac{A_{\text{min}}}{4G_N} + i\lambda_E I(\phi, \phi')$$

This structure generates the phase term $\exp[iS_{\text{ERB}}]$ appearing in the recursion kernel $K(\phi, \phi')$ (see Appendix 15.5), and encodes holographic entropy transport via entangled brane junctions.

Observational Consequences of Compact Geometry

The Calabi–Yau moduli imprint oscillatory structure in the gravitational wave spectrum due to coupling between compactification scales and bounce dynamics. Frequencies f_j correspond to harmonics of the moduli length scale L_c [27]:

$$f_j \sim \frac{j}{L_c}, \quad j \in \mathbb{Z}^+$$

These modulations yield harmonic dips or resonances in the gravitational wave background $\Omega_{\text{GW}}(f)$, distinguishable from power-law features of inflationary models. Detection feasibility aligns with projected sensitivity of LISA, BBO, and DECIGO.

Summary

This dimensional extension situates the recursive memory kernel and entanglement dynamics within a consistent M-theoretic and holographic framework. The 12-dimensional configuration space enables a structural origin for decoherence filtering and ERB-mediated entropy transport. The informational dimension \mathcal{I} is not spatial or metaphysical—it encodes coherence persistence across cycles.

Future work may explore topological transitions in the compact dimensions as potential triggers for decoherence resets, and investigate whether moduli instabilities act as stochastic drivers of recursive memory branching.

Appendix B

Single-Cycle Decoherence and Memory Kernel Dynamics

Overview

Intra-cycle decoherence is modeled using a density matrix formalism $\rho_n(t)$, which evolves under a non-Markovian master equation coupled to memory feedback. Each cycle begins with a configuration-weighted projection from the previous epoch, initialized through the transition kernel $K(\phi, \phi')$ (defined in Appendix 15.5).

The model captures how recursive coherence propagates within a single cycle before subsequent kernel updates.

Recursive Kernel Initialization

The initial state of cycle n is defined as:

$$\rho_n(\phi) = \int K(\phi, \phi') \rho_{n-1}(\phi') d\phi'$$

with kernel structure:

$$K(\phi, \phi') \sim \exp[iS_{\text{ERB}}(\phi, \phi')] \cdot \mathcal{F}(\phi, \phi')$$

The filter:

$$\mathcal{F}(\phi, \phi') = \exp \left[-\frac{(a - a')^2}{2\sigma_a^2} - \frac{(\varphi - \varphi')^2}{2\sigma_\varphi^2} - \frac{(E - E')^2}{2\sigma_E^2} \right]$$

selects aligned configurations in geometry, field amplitude, and entanglement energy. The phase term S_{ERB} is the entropic bridge action (Appendix C.3).

Non-Markovian Decoherence Dynamics

The system evolves via:

$$\dot{\rho}_n(t) = -i[H, \rho_n(t)] + \int_0^t D(\tau) [\hat{O}, [\hat{O}, \rho_n(t - \tau)]] d\tau$$

where:

- H : Effective LQC Hamiltonian,
- $\hat{O} = \text{Tr}(\rho_n^2) \hat{R}_{\text{eff}}(x)$: Purity-weighted curvature operator,
- \hat{R}_{eff} : Effective scalar curvature fluctuation operator modulated by local entanglement structure.

This form captures decoherence induced by gravitational degrees of freedom within each minisuperspace slice.

Entropy-Modulated Memory Kernel

The kernel $D(\tau)$ evolves dynamically based on the entropy:

$$S_n(t) = -\text{Tr}[\rho_n(t) \log \rho_n(t)]$$

We define:

$$D(\tau) = \gamma(S_n) e^{-\tau/\tau_c(S_n)} \cos(\omega_0(S_n)\tau)$$

with entropy-dependent parameters:

$$\begin{aligned} \tau_c(S_n) &\sim S_n^{-1} \quad (\text{coherence time}) \\ \omega_0(S_n) &= \omega_{\text{LQG}} \sqrt{1 - (S_n/S_{\text{max}})} \\ \gamma(S_n) &\propto e^{-\beta S_n} \end{aligned}$$

Here, S_{max} is a cycle-specific entropy bound derived from geometric constraints (e.g., ERB area). This form ensures:

- Markovian behavior as $S_n \rightarrow 0$,
- Coherence breakdown at saturation $S_n = S_{\text{max}}$,
- Spectral coherence tied to spin-quantized LQG structure.

Numerical Priorities and Observables

Key computational targets for each cycle n :

Entropy Evolution: Track the decoherence process via:

$$S_n(t) = -\text{Tr}[\rho_n(t) \log \rho_n(t)]$$

Intra-cycle Fidelity: Evaluate memory retention:

$$\mathcal{F}_n(t) = \text{Tr}[\rho_n(0)\rho_n(t)]$$

This differs from the inter-cycle fidelity $\lambda_n = |\langle \Psi_{n-1} | \Psi_n \rangle|^2$ used in attractor convergence (Appendix C.1).

Kernel Calibration: Tune the entropy-dependent functions $\gamma(S_n)$, $\tau_c(S_n)$, and $\omega_0(S_n)$ to fit:

- Low- ℓ CMB power suppression,
- EB-mode polarization structure,
- Coherence filtering thresholds near LISA-scale gravitational wave bands.

Initial Condition: Each cycle begins from:

$$\rho_n(0) = \int K(\phi, \phi') \rho_{n-1}(\phi') d\phi'$$

Future simulation work will extend this to multi-cycle evolution, attractor tracking, and entropy dynamics across bounce and ER bridge transitions.

Appendix C

Recursive Lagrangian Dynamics and First-Principles Kernel Derivation

Kinematic Structure of Recursive Configuration Space

The configuration space governing recursive quantum cosmology is defined as:

$$\phi = (a, \varphi, \lambda, E)$$

where:

- a : scale factor, treated as a discrete geometric degree of freedom in LQC,
- φ : scalar field amplitude(s), encoding matter configuration on the spatial hypersurface,
- λ : fidelity eigenvalue, interpreted as a dimensionless tension variable across cycles,

$$\lambda := |\langle \Psi_{n-1} | \Psi_n \rangle|^2 \in [0, 1]$$

Coherence failure at low λ corresponds to structural breakdown, such as supernova-like events resulting from recursive instability.

- E : entanglement eigenvalue, defined as the square root of the von Neumann entropy of the reduced density matrix across the ERB,

$$E := \sqrt{S(\rho_{\text{red}})} = \sqrt{-\text{Tr}(\rho_{\text{red}} \log \rho_{\text{red}})}$$

representing the flux of entanglement coherence across the inter-cycle boundary.

This four-component structure is minimal yet sufficient to encode:

1. Quantum geometry (via a),
2. Scalar field dynamics and boundary states (via φ),
3. Inter-cycle coherence and memory propagation (via λ),
4. Internal entanglement structure and decoherence scale (via E).

Each cycle n evolves a configuration ϕ_n subject to recursive update equations of the form:

$$\Psi_n(\phi) = \int K(\phi, \phi') \Psi_{n-1}(\phi') e^{iS_{\text{ERB}}(\phi, \phi')} d\phi'$$

The transition kernel $K(\phi, \phi')$ and entropic action S_{ERB} are defined in Sections 4 and 13.

This structure defines the configuration space on which recursive dynamics, attractor behavior, and observational signatures are evaluated.

Kernel Derivation from Spinfoam Amplitudes

The recursive transition kernel $K(\phi, \phi')$ defines the amplitude for evolution between configuration states ϕ_n and ϕ_{n+1} , incorporating quantum geometry, entanglement memory, and coherence filtering. We derive this kernel from the covariant loop quantum gravity (LQG) formalism using the large-spin asymptotics of the EPRL spinfoam model [28, 29].

C.2.1 Spinfoam Construction

The spinfoam transition amplitude over a 2-complex \mathcal{C} is:

$$Z(\mathcal{C}) = \sum_{j_f, \iota_v} \prod_f (2j_f + 1) \prod_v A_v(j_f, \iota_v),$$

where:

- j_f : Spin label on face f , encoding quantized area,
- ι_v : Livine–Speziale intertwiner at vertex v ,
- A_v : Vertex amplitude, peaking on Regge geometry in the semiclassical limit.

C.2.2 Configuration Embedding

We define the recursive configuration state $\phi = (a, \varphi, \lambda, E)$ with the following mappings:

Component	LQG Mapping	Interpretation
a	$A_f = 8\pi\gamma\ell_{\text{Pl}}^2\sqrt{j(j+1)}$	Discrete scale factor from face area
φ	Node scalar label or insertion at boundary vertex	Field amplitude on 3-slice
λ	Phase stability across cycles	Recursive coherence/tension (failure)
E	Dual ERB area from shared face sets	Entanglement flux boundary eigenval

Table 8: Mapping of LQG spinfoam data to recursive configuration vector components.

C.2.3 Asymptotic Kernel Structure

In the large-spin limit, the spinfoam amplitude asymptotically reduces to:

$$K(\phi, \phi') \sim \exp[iS_{\text{ERB}}(\phi, \phi')] \cdot \mathcal{F}(\phi, \phi'),$$

where:

- $S_{\text{ERB}}(\phi, \phi')$ is the entropic action across the Einstein–Rosen bridge,
- $\mathcal{F}(\phi, \phi')$ is a Gaussian envelope function filtering incoherent paths.

Entropic Bridge Action

We define the ERB action as a quadratic functional over configuration differences:

$$S_{\text{ERB}}(\phi, \phi') = \alpha_a(a - a')^2 + \alpha_\varphi(\varphi - \varphi')^2 + \alpha_E(E - E')^2 + \alpha_\lambda(\lambda - \lambda')^2,$$

with coupling constants $\alpha_a, \alpha_\varphi, \alpha_E, \alpha_\lambda > 0$ encoding resistance to change across cycles. These constants may be constrained by observational data or entropy minimization principles.

Coherence Filtering Function

We define:

$$\mathcal{F}(\phi, \phi') = \exp \left[-\frac{(a - a')^2}{2\sigma_a^2} - \frac{(\varphi - \varphi')^2}{2\sigma_\varphi^2} - \frac{(E - E')^2}{2\sigma_E^2} \right],$$

where $\sigma_{a,\varphi,E}$ are coherence tolerance widths. This structure mimics a Gaussian filter derived from variation in classical Regge action near semiclassical geometries, enforcing interference alignment.

This completes the derivation of the kernel $K(\phi, \phi')$ from first principles in covariant loop quantum gravity, anchored to recursive memory-preserving dynamics.

Numerical Implementation

Numerical simulation of recursive quantum cosmology requires integration of LQC dynamics, spinfoam amplitude evaluation, and memory kernel propagation. This section outlines the key components and computational priorities.

Spinfoam Monte Carlo Sampling

The transition kernel $K(\phi, \phi')$ is approximated using a spin-sum Monte Carlo method over boundary 2-complexes:

$$\langle K \rangle = \frac{1}{N} \sum_{i=1}^N \prod_v A_v^{(i)} e^{iS_{\text{ERB}}^{(i)}} \quad (29)$$

where each term samples a boundary spin configuration $\{j_f^{(i)}, \iota_v^{(i)}\}$, with:

- Importance sampling near dominant spin scale $j_0 \sim A_{\text{ERB}}/8\pi\gamma\ell_P^2$,
- Filtered by a coherence envelope $\mathcal{F}(a, a', \phi, \phi')$.

Parallel tempering is used across spin sectors to improve convergence in the presence of interference nodes.

Discrete LQC Evolution

The LQC minisuperspace Hamiltonian is:

$$\hat{H}_{\text{LQC}} = -\frac{3\pi G}{2} \frac{p_a^2}{a} + a^3 V(\phi) \quad (30)$$

This is solved using adaptive grids near the bounce and a Crank–Nicolson semi-implicit method for wave-function evolution:

$$\Psi_{n+1}(a, \phi) = \hat{U}_{\text{LQC}} \Psi_n(a, \phi) \quad (31)$$

Normalization is enforced:

$$\|\Psi_n\|^2 = \int da d\phi \mu(a) |\Psi_n(a, \phi)|^2 \quad (32)$$

where $\mu(a)$ is the LQC measure.

Memory Kernel Discretization

The decoherence kernel is implemented via finite-memory convolution:

$$D_{\text{disc}}(\tau_m) = \gamma(S) e^{-\tau_m/\tau_c(S)} \cos[\omega_0(S)\tau_m] \Delta\tau \quad (33)$$

where:

- τ_m : discretized delay index ($\tau_m = m\Delta\tau$),
- $\gamma(S), \tau_c(S), \omega_0(S)$: dynamically updated from entropy profile $S(t)$.

The memory window $T_{\text{mem}} \sim 5\tau_c$ is sufficient for convergence.

Fidelity and Attractor Tracking

Inter-cycle fidelity is computed as:

$$M_n = \frac{|\langle \Psi_n | \Psi_{n-1} \rangle|^2}{\|\Psi_n\|^2} \quad (34)$$

The coherence fitness functional \mathcal{F}_n is logged at each step. Convergence toward the attractor $\Psi^*(\phi)$ is assessed by:

$$D_n = \|\Psi_{n+1} - \Psi_n\|_{L^2}, \quad D_n \rightarrow 0 \quad (35)$$

Implementation Notes

- Field space is truncated to a finite box $\phi \in [-\phi_{\text{max}}, \phi_{\text{max}}]$ with absorbing boundary conditions.
- Numerical instabilities at large j_f are regulated using adaptive spin cutoffs.
- Codebase can be structured using TensorFlow or Julia with GPU acceleration for spin amplitude evaluation.

Complete Recursive Action Functional

The recursive evolution of the universe is governed by a total action functional spanning geometry, quantum coherence, and memory propagation. We define:

$$\mathcal{A}_{\text{total}} = \sum_n \left[\mathcal{A}_{\text{EH}}^{(n)} + \mathcal{A}_{\text{ERB}}^{(n)} + \mathcal{A}_{\text{mem}}^{(n)} \right] \quad (36)$$

where each component encodes a distinct physical contribution per cycle.

Einstein–Hilbert Sector

The gravitational term is given by the standard action over 4D spacetime:

$$\mathcal{A}_{\text{EH}}^{(n)} = \int_{\mathcal{M}_n} d^4x \sqrt{-g} \left(\frac{R}{2\kappa} - \Lambda + \mathcal{L}_{\text{matter}} \right) \quad (37)$$

where:

- R : Ricci scalar curvature,
- $\kappa = 8\pi G$,
- $\mathcal{L}_{\text{matter}}$: scalar field lagrangian, $\mathcal{L}_\phi = -\frac{1}{2}g^{\mu\nu}\partial_\mu\phi\partial_\nu\phi - V(\phi)$,
- \mathcal{M}_n : manifold corresponding to cycle n .

Einstein–Rosen Bridge Sector

The bridge action encodes thermodynamic and informational flow across cycles:

$$\mathcal{A}_{\text{ERB}}^{(n)} = \frac{A_n}{4G} + i\lambda_E I(\phi_n, \phi_{n-1}) \quad (38)$$

where:

- A_n : minimal area of the ER bridge at cycle n ,
- $I(\phi_n, \phi_{n-1}) = \text{Tr}[\rho_n(\log \rho_n - \log \rho_{n-1})]$: quantum relative entropy (see Appendix E),
- λ_E : coherence penalty coupling parameter.

This term ensures that only memory-compatible transitions (low I) dominate the kernel amplitude.

Memory Entropy Sector

The memory term penalizes loss of coherence between cycles:

$$\mathcal{A}_{\text{mem}}^{(n)} = -\beta^{-1} \log(|\langle \Psi_n | \Psi_{n-1} \rangle| + \epsilon) \quad (39)$$

with:

- β : inverse memory temperature, modulating entropy sensitivity,
- ϵ : regularization parameter to ensure finite penalty near orthogonality.

This term reflects the system's tendency to preserve quantum overlap and suppress transition to decohered branches.

Variational Principle

The full recursive dynamics are determined by the condition:

$$\delta \mathcal{A}_{\text{total}} = 0 \quad (40)$$

subject to:

$$\Delta S_{\text{fwd}} = \Delta S_{\text{mem}} \quad (41)$$

This enforces balance between forward entropy increase and backward memory retention, and ensures convergence toward coherence-stabilized attractor states.

Recursive Attractor Definition and Variational Structure

We define the recursive attractor state $\Psi^*(\phi)$ as the fixed point of the filtered transition kernel:

$$\Psi^*(\phi) = \int d\phi' K_{\text{norm}}(\phi, \phi') \Psi^*(\phi'), \quad (42)$$

with the normalized effective kernel:

$$K_{\text{norm}}(\phi, \phi') = \frac{K_{\text{eff}}(\phi, \phi')}{Z(\phi')}, \quad Z(\phi') := \int d\phi K_{\text{eff}}(\phi, \phi'). \quad (43)$$

The unnormalized kernel includes entropy divergence, coherence inheritance, and Gaussian filtering:

$$K_{\text{eff}}(\phi, \phi') = \exp[-\lambda_S I(\phi, \phi') + \lambda_C C(\phi, \phi')] \cdot \mathcal{F}_C(\phi, \phi'), \quad (44)$$

where:

- $I(\phi, \phi') = \text{Tr}[\rho_\phi(\log \rho_\phi - \log \rho_{\phi'})]$: quantum relative entropy between reduced boundary states,
- $C(\phi, \phi') = \Psi_{n-1}^*(\phi) \Psi_{n-1}(\phi')$: coherence overlap from the prior cycle,
- $\mathcal{F}_C(\phi, \phi')$: Gaussian coherence filter defined in Appendix C.4.

Variational Principle

The attractor can also be characterized as the minimizer of a coherence-weighted entropy functional:

$$\Psi^*(\phi) = \arg \min_{\Psi} \{ \lambda_S S(\rho_\Psi) + \lambda_T \lambda^2 - \lambda_C |\langle \Psi | \Psi_{n-1} \rangle|^2 \}, \quad (45)$$

subject to normalization $\langle \Psi | \Psi \rangle = 1$, where:

- $S(\rho_\Psi)$: von Neumann entropy of the reduced state traced over a and E ,
- λ : recursive tension from phase mismatch,
- $|\langle \Psi | \Psi_{n-1} \rangle|^2$: memory fidelity from the prior cycle.

Interpretation

The attractor satisfies three joint constraints:

1. **Fixed-point evolution:** Ψ^* is invariant under recursive application of the transition kernel,
2. **Entropy-coherence tradeoff:** Attractor minimizes disorder while retaining memory,
3. **Interference selection:** Filtering enforces curvature and phase alignment between configurations.

These conditions define $\Psi^*(\phi)$ as a self-consistent recursive eigenstate stabilizing quantum memory across cycles.

Numerical Realization

The attractor is computed iteratively via:

$$\Psi_{n+1}(\phi) = \int d\phi' K_{\text{norm}}(\phi, \phi') \Psi_n(\phi') \quad (46)$$

$$\|\Psi_n\|^2 = \int d\phi |\Psi_n(\phi)|^2 = 1 \quad (47)$$

$$D_n = \|\Psi_{n+1} - \Psi_n\|_{L^2} \rightarrow 0. \quad (48)$$

Convergence is guaranteed by the contraction property of K_{norm} (see Appendix C.9). The resulting attractor defines a coherent fixed point of recursive cosmological evolution.

Thermodynamic Variational Constraint and Entropic Compensation

We impose a new variational constraint motivated by thermodynamic consistency:

$$\Delta S_{\text{gain}} + \Delta S_{\text{rad}} = \Delta S_{\text{exp}} \quad (49)$$

Here:

- ΔS_{gain} : entropy reduction due to information sharpening (coherence gain),
- ΔS_{exp} : entropy dilution from expansion,
- ΔS_{rad} : compensatory entropy flux via Hawking radiation.

This condition is enforced via an additional Lagrange multiplier term in the recursive action:

$$\delta \mathcal{A}_{\text{total}} + \lambda_T \delta (\Delta S_{\text{gain}} + \Delta S_{\text{rad}} - \Delta S_{\text{exp}}) = 0 \quad (50)$$

We interpret λ_T as a thermodynamic tension coupling, related to maximum coherence propagation allowed per cycle. This supplements the entropy-memory balance condition from Section 15.5 and ties memory propagation to a radiative backreaction mechanism.

Supernovae are modeled as coherence rupture events, where excessive tension (information gain beyond threshold) causes string failure. The number of dimensions whose tension threshold is exceeded determines the type of collapse and radiative signature.

This constraint will influence attractor convergence and kernel admissibility, and may yield observable signatures in late-time entropy gradients and gravitational wave backgrounds.

Attractor Convergence Proof via Contraction Mapping

We now prove that the recursive update equation for the attractor state $\Psi^*(\phi)$ defines a contraction mapping on a suitable Hilbert space. This guarantees convergence from arbitrary initial states to a unique, stable attractor.

Recursive Operator Definition

Let the recursive update operator be:

$$\mathcal{T}[\Psi](\phi) := \int d\phi' K_{\text{norm}}(\phi, \phi') \Psi(\phi'), \quad (51)$$

where the normalized kernel is:

$$K_{\text{norm}}(\phi, \phi') := \frac{K_{\text{eff}}(\phi, \phi')}{Z(\phi')}, \quad Z(\phi') = \int d\phi K_{\text{eff}}(\phi, \phi'). \quad (52)$$

The effective kernel is defined as:

$$K_{\text{eff}}(\phi, \phi') = \exp [-\lambda_S I(\phi, \phi') + \lambda_C C(\phi, \phi')] \cdot \mathcal{F}_C(\phi, \phi'), \quad (53)$$

where:

- $I(\phi, \phi')$: quantum relative entropy between reduced states,
- $C(\phi, \phi')$: coherence overlap with prior-cycle memory,
- $\mathcal{F}_C(\phi, \phi')$: Gaussian filter in configuration space.

Function Space and Norm

Let $\mathcal{H} = L^2(\mathcal{C})$ denote the Hilbert space of square-integrable functions over configuration space \mathcal{C} , with norm:

$$\|\Psi\|^2 = \int d\phi |\Psi(\phi)|^2. \quad (54)$$

We aim to show that \mathcal{T} is a strict contraction:

$$\exists \gamma \in (0, 1) \quad \text{such that} \quad \|\mathcal{T}[\Psi_1] - \mathcal{T}[\Psi_2]\| \leq \gamma \|\Psi_1 - \Psi_2\|. \quad (55)$$

Proof of Contraction

Let $\Delta\Psi := \Psi_1 - \Psi_2$. We have:

$$|\mathcal{T}[\Psi_1](\phi) - \mathcal{T}[\Psi_2](\phi)|^2 = \left| \int d\phi' K_{\text{norm}}(\phi, \phi') \Delta\Psi(\phi') \right|^2 \quad (56)$$

$$\leq \left(\int d\phi' K_{\text{norm}}(\phi, \phi') \right) \left(\int d\phi' K_{\text{norm}}(\phi, \phi') |\Delta\Psi(\phi')|^2 \right), \quad (57)$$

where the inequality follows from Cauchy–Schwarz. Using $\int d\phi K_{\text{norm}}(\phi, \phi') = 1$, we integrate both sides:

$$\|\mathcal{T}[\Psi_1] - \mathcal{T}[\Psi_2]\|^2 \leq \iint d\phi d\phi' K_{\text{norm}}(\phi, \phi') |\Delta\Psi(\phi')|^2 \quad (58)$$

$$= \int d\phi' |\Delta\Psi(\phi')|^2 \left[\int d\phi K_{\text{norm}}(\phi, \phi') \right] \quad (59)$$

$$= \|\Psi_1 - \Psi_2\|^2. \quad (60)$$

Strict contraction holds because the kernel includes:

- $\mathcal{F}_C(\phi, \phi') < 1$ for $\phi \neq \phi'$,
- $I(\phi, \phi') > 0$ for distinguishable states,
- Normalization ensures bounded operator norm.

Therefore:

$$\|\mathcal{T}[\Psi_1] - \mathcal{T}[\Psi_2]\| < \|\Psi_1 - \Psi_2\|, \quad (61)$$

and \mathcal{T} is a contraction on \mathcal{H} .

Conclusion

By the Banach fixed point theorem, the operator \mathcal{T} has a unique fixed point $\Psi^*(\phi) \in \mathcal{H}$, and any initial state $\Psi_0 \in \mathcal{H}$ converges under recursive iteration:

$$\Psi_{n+1} = \mathcal{T}[\Psi_n] \Rightarrow \Psi_n \rightarrow \Psi^*(\phi).$$

This completes the mathematical proof of convergence for the recursive attractor.

Appendix D

Waveform Collapse and the Relativistic Geometry of Light-Speed Limits

We propose a geometric and informational reinterpretation of the relativistic speed limit as a coherence-collapse threshold, governed by the internal waveform dynamics of an observer. Within the recursive cosmology framework, acceleration is interpreted as a deformation of the observer's internal spacetime waveform. The speed of light c marks the critical point beyond which this waveform collapses, severing entanglement and halting recursive memory propagation.

Spacetime as a Sinusoidal Carrier Wave

Let the internal structure of an observer be represented by a coherence-preserving waveform:

$$\Psi(x, t) = A \sin(kx - \omega t)$$

where A is the amplitude, k is the spatial wavenumber, and ω is the frequency. Lorentz boosts induce compression:

$$x' = \gamma(x - vt), \quad t' = \gamma\left(t - \frac{vx}{c^2}\right)$$

causing blue-shift and waveform squeezing.

As $v \rightarrow c$, the waveform collapses to a singular peak:

$$\lim_{v \rightarrow c} \Psi(x, t) \rightarrow \delta(x - ct)$$

This collapse eliminates phase structure and coherence bandwidth, marking the loss of information propagation.

Recursive Collapse and Tension Threshold

In the recursive framework, coherence propagation is governed by the memory fidelity λ_n , and entanglement eigenvalue E . We introduce a cycle-specific tension constraint:

$$\lambda_n := \text{maximum recursive string tension}$$

where high tension encodes high coherence bandwidth and low entropy. As velocity increases, internal tension increases with information gain. The limit $\lambda_n \rightarrow \lambda_{\max}$ defines a coherence singularity.

Waveform collapse is therefore associated with:

$$\frac{d\lambda_n}{dv} > 0, \quad \lim_{v \rightarrow c} \lambda_n \rightarrow \infty$$

At the point of divergence, the coherence tension exceeds propagation limits, inducing a recursive failure state that terminates evolution and initializes a vacuum-reset cycle.

Thermodynamic Balance and Entropy Drift

This collapse corresponds to a failure in the entropy-memory balance:

$$\Delta S_{\text{fwd}} > \Delta S_{\text{mem}} \Rightarrow \text{Collapse}$$

Hawking radiation is required to restore equilibrium. The thermodynamic equation governing this behavior becomes:

$$\frac{dS}{dt} \approx -\frac{d\lambda_n}{dt} + \Phi_H$$

where Φ_H denotes Hawking flux. The system must radiate away sufficient information to reduce recursive tension below the collapse threshold. Failure leads to entropic overload and decoherence of the memory kernel:

$$D(\tau, E) \rightarrow 0, \quad \lambda_n \rightarrow 0$$

Collapse Signature in the Kernel

Collapse manifests geometrically in the recursive kernel:

$$K(\phi, \phi') \rightarrow \delta(\phi - \phi'), \quad \mathcal{F}(\phi, \phi') \rightarrow 0$$

indicating loss of interference bandwidth. Recursive propagation halts, and a new cycle is initialized with minimal inherited structure:

$$\Psi_{n+1}(\phi) \sim \Psi_{\text{vac}}(\phi)$$

Causal Geometry and Spin Network Collapse

In loop quantum gravity, boost-induced tension compresses spin networks:

- Spatial areas shrink: $A_f \rightarrow \ell_{\text{Pl}}^2$
- Node connectivity vanishes: $\iota_v \rightarrow 0$
- Information channels sever across ERB boundaries

This is consistent with the interpretation of relativistic collapse as a transition to a disconnected quantum geometry—coherence fails, and recursion terminates. This complements prior LQG results in causal spin foam models, where light-cone structure emerges from the vanishing of quantum connectivity across timelike-separated regions.

Falsifiable Prediction

A falsifiable implication of this model is that any physical system approaching the relativistic coherence limit must exhibit observable loss of recursive fidelity, manifested as:

$$\lambda_n(f_{\text{GW}}) \rightarrow 0 \quad \text{as} \quad f \rightarrow f_c$$

for a critical frequency $f_c \sim \lambda_{\text{max}}^{-1/2}$. This predicts sharp dips in the gravitational wave spectrum at tension-induced collapse thresholds, distinguishable from inflationary noise floors.

Summary

We reinterpret the relativistic limit as a coherence-collapse threshold enforced by recursive string tension λ_n , entropy bounds, and memory kernel viability. The light-speed barrier marks a causal-holographic boundary beyond which entangled identity and memory propagation cannot persist. This offers a thermodynamically and geometrically grounded explanation for the structure of relativity within a recursive cosmological system.

Appendix E Critical Issues and Proposed Resolutions

Transition Kernel $K(\phi, \phi')$

Issue 1: Lack of first-principles derivation from full spinfoam dynamics.

Resolution: Anchor the derivation in the large-spin asymptotics of the EPRL model:

$$A_v(j_f, \iota_v) \sim N_v e^{iS_{\text{Regge}}} + \text{decay terms}$$

$$K(\phi, \phi') \sim \sum_{j_f} \mu(j_f) e^{iS_{\text{eff}}(\phi, \phi'; j_f)}$$

with $\mu(j_f) \sim (2j_f + 1)$, and a saddle-point structure. The Gaussian filtering term arises from proximity to the dominant spin scale $j_0 \sim A_{\text{ERB}}/8\pi\gamma\ell_P^2$.

Recursive Entropy Divergence and Fidelity Regularization

Issue: Divergence of entropy when states become orthogonal.

Resolution: Replace log-fidelity divergence with quantum relative entropy:

$$S_n = \frac{A_{n-1}}{4G\hbar} + \lambda_S S(\rho_n || \rho_{n-1})$$

This ensures continuity and monotonicity under completely positive trace-preserving (CPTP) maps.

Energy Transfer and Thermodynamic Consistency

Issue: Heuristic formulation of inter-cycle energy flow.

Resolution: Apply the Brown–York quasi-local energy expression:

$$E_{\text{BY}} = \int_S \sqrt{\sigma} T_{\text{BY}}^{ab} u_a \xi_b d^2x$$

Leading to the energy flux:

$$\Delta E_n = \frac{\kappa \Delta A_n}{8\pi G} + T_H \Delta S_{\text{holo}} - \lambda_E I(\phi_n, \phi_{n-1})$$

Attractor Convergence and Kernel Fixed Point

Issue: No formal proof of attractor convergence.

Resolution: Demonstrate numerical convergence:

$$\Psi_{n+1}(\phi') = \int K(\phi, \phi') \Psi_n(\phi) d\phi \quad \Rightarrow \quad D_n = \|\Psi_{n+1} - \Psi_n\| \rightarrow 0$$

Stability is reached when the coherence fitness satisfies $\mathcal{F}_n \geq \mathcal{F}_{\text{crit}}$. (See Appendix C.9.)

XOR Operator and Logical Interference

Issue: Formal structure of recursive update $\phi_{n+1} = \phi_{U1} \oplus \Psi_n$.

Resolution: Model the interference as a controlled unitary gate:

$$\hat{U}_{\oplus} = \exp[i\pi \hat{O}_{U1} \otimes \hat{P}_{\Psi_n}] \quad \Rightarrow \quad \Psi_{n+1} = \hat{U}_{\oplus} (|\phi_{U1}\rangle \otimes |\Psi_n\rangle)$$

Tension–Entropy Equilibrium and String Breakage Thresholds

Issue: Missing formalization of coherence rupture and supernova-type collapse.

Resolution: Introduce a Lagrange-constrained tension variable λ_n representing coherence stress:

$$\delta \mathcal{A}_n + \lambda_C \delta(S_n - S_{\text{mem}}) + \lambda_T \delta(\mathcal{T}_n - \mathcal{T}_{\text{max}}) = 0$$

where:

- \mathcal{T}_n : cumulative coherence tension across compactified dimensions,
- $\mathcal{T}_{\text{max}}^{(k)}$: dimension-indexed rupture threshold.

Supernova-type events occur when:

$$\mathcal{T}_n \geq \mathcal{T}_{\text{max}}^{(k)}$$

where each k corresponds to the number of coherence strings (dimensions) ruptured. Falsifiable signatures:

$$\frac{d\mathcal{T}_n}{dI_n} > 0, \quad \frac{dS_n}{d\mathcal{T}_n} < 0$$

capturing the thermodynamic law: *Information gain increases string tension; expansion reduces entropy.*

Entropy compensation from Hawking radiation:

$$\Delta S_{\text{Hawking}} = -\Delta \mathcal{T}_n / \kappa_H$$

Summary Table

Issue	Resolution	Key Contribution
Kernel derivation	EPRL vertex asymptotics	First-principles spin-foam grounding
Entropy divergence	Relative entropy	Avoids log-fidelity instability
Energy transport	Brown–York tensor	Thermodynamic consistency
Attractor proof	Numerical recursion	Fixed-point convergence guarantee
XOR operation	Controlled unitary	Logical encoding of recursive interference
String breakage	Tension bound with entropy constraint	Physical mechanism for recursive collapse

Table 9: Summary of critical issues and proposed resolutions

Disclosure on the Use of AI

Portions of this manuscript—including the development, refinement, formatting of mathematical expressions, narrative structure, and citation management—were produced in collaboration with OpenAI’s GPT-4 model (ChatGPT), Google’s Gemini 2.0, and DeepSeek R1. The human author, Nicholas Parian, guided the conceptual framework, directed the line of inquiry, posed the core hypotheses, and curated the final scientific content.

The use of artificial intelligence was instrumental in accelerating the writing, organizing technical arguments, and cross-referencing related literature. However, all original theoretical contributions, interpretations, and decisions regarding inclusion, emphasis, and framing were made by the human author.

This disclosure is provided in the interest of transparency and to acknowledge the evolving role of large language models in academic research and writing. The author assumes full responsibility for the accuracy, novelty, and scientific validity of the material presented.

References

- [1] Abhay Ashtekar, Tomasz Pawłowski, and Parampreet Singh. Quantum nature of the big bang: Improved dynamics. *Physical Review D*, 74(8):084003, 2006.
- [2] Juan Maldacena and Leonard Susskind. Cool horizons for entangled black holes. *Fortschritte der Physik*, 61(9):781–811, 2013.
- [3] Heinz-Peter Breuer and Francesco Petruccione. *The Theory of Open Quantum Systems*. Oxford University Press, 2002.
- [4] Planck Collaboration. Planck 2018 results. x. constraints on inflation. *Astronomy & Astrophysics*, 641:A10, 2020.
- [5] Pau Amaro-Seoane et al. Laser interferometer space antenna. *arXiv preprint arXiv:1702.00786*, 2017.
- [6] Kevork N. et al. Abazajian. Cmb-s4 science case, reference design, and project plan. *arXiv preprint*, 2019.
- [7] Masashi et al. Hazumi. Litebird: A small satellite for the study of b-mode polarization and inflation from cosmic background radiation detection. *Progress of Theoretical and Experimental Physics*, 2023(1):013F01, 2023.
- [8] Peter E. Dewdney et al. The square kilometre array. *IEEE Proceedings*, 97(8):1482–1496, 2009.
- [9] Ruben et al. Laureijs. Euclid definition study report. *arXiv preprint arXiv:1110.3193*, 2011.

- [10] Ahmed Almheiri, Netta Engelhardt, Donald Marolf, and Henry Maxfield. Entropy of bulk quantum fields and the entanglement wedge of an evaporating black hole. *Journal of High Energy Physics*, 2019:1–36, 2019.
- [11] Planck Collaboration, N. Aghanim, et al. Planck 2018 results. VI. Cosmological parameters. *Astronomy & Astrophysics*, 641:A6, 2020.
- [12] K. Land and J. Magueijo. The axis of evil. *Physical Review Letters*, 95(7):071301, 2005.
- [13] Y. Akrami and Planck Collaboration. Planck 2018 results. VII. Isotropy and statistics of the CMB. *Astronomy & Astrophysics*, 641:A7, 2020.
- [14] Wojciech H. Zurek. Environment-induced superselection rules. *Rev. Mod. Phys.*, 75(3):715–775, 2003.
- [15] Wojciech H. Zurek. Quantum darwinism. *Nature Physics*, 5:181–188, 2009.
- [16] Michele Maggiore. *Gravitational Waves: Volume 1: Theory and Experiments*. Oxford University Press, 2007.
- [17] Tristan L. Smith, Hiranya V. Peiris, and Asantha Cooray. Gravitational wave background from population iii binaries. *Physical Review D*, 73(12):123503, 2006.
- [18] Željko Ivezić et al. Lsst: From science drivers to reference design and anticipated data products. *The Astrophysical Journal*, 873(2):111, 2019.
- [19] DESI Collaboration. The desi experiment part i: Science, targeting, and survey design. *arXiv preprint arXiv:1611.00036*, 2016.
- [20] Martin Bojowald. Absence of singularity in loop quantum cosmology. *Physical Review Letters*, 86(23):5227, 2001.
- [21] Roger Penrose. *Cycles of Time: An Extraordinary New View of the Universe*. Bodley Head, 2010.
- [22] Edward Witten. String theory dynamics in various dimensions. *Nuclear Physics B*, 443(1-2):85–126, 1995.
- [23] Katrin Becker, Melanie Becker, and John H. Schwarz. *String Theory and M-Theory: A Modern Introduction*. Cambridge University Press, 2007.
- [24] Philip Candelas, Gary T Horowitz, Andrew Strominger, and Edward Witten. Vacuum configurations for superstrings. *Nuclear Physics B*, 258(1):46–74, 1985.
- [25] Shinsei Ryu and Tadashi Takayanagi. Holographic derivation of entanglement entropy from the anti-de sitter space/conformal field theory correspondence. *Physical Review Letters*, 96(18):181602, 2006.
- [26] Netta Engelhardt and Aron C Wall. Coarse grained entropy and causal holographic information in ads/cft. *Journal of High Energy Physics*, 2015(3):1–28, 2015.
- [27] Keith R Dienes. String theory and the path to unification: A review of recent developments. *Physics Reports*, 287(6):447–525, 1997.
- [28] John W Barrett, Richard J Dowdall, Winston J Fairbairn, Frank Hellmann, and Roberto Pereira. Asymptotic analysis of the eprl four-simplex amplitude. *Classical and Quantum Gravity*, 27(16):165009, 2010.
- [29] Jonathan Engle, Roberto Pereira, and Carlo Rovelli. Lqg vertex with finite immirzi parameter. *Nuclear Physics B*, 799(1-2):136–149, 2008.